2Mij

Thermally Driven Mass Flows In the

Convection Zone of the Sun

by

Geert C. Dijkhuis

SUIPR Report No. 518

May 1973

REPRODUCTION RESTRICTIONS OVERRIDDEN

INSTITUTE FOR PLASMA RESEARCH
STANFORD UNIVERSITY, STANFORD, CALIFORNIA

THERMALLY DRIVEN MASS FLOWS IN THE CONVECTION
ZONE OF THE SUN

by

Geert C. Dijkhuis

SUIPR Report No. 518

May 1973

Institute for Plasma Research
Stanford University
Stanford, California

j

© Copyright 1973

by

Geert Cornelis Dijkhuis

ii

$$\ldots \pi\alpha\nu\tau\alpha \ \rho\epsilon\iota \ldots$$

Heraclitus, 600 B.C.

ABSTRACT

In this dissertation a formulation of the fluid dynamics of convective regions is developed which leads to an analytical description of the solar rotation, the Evershed flow and the supergranulation. The starting point of the present formulation is the mixing length picture of convective equilibrium, but the earlier point mass model for convective molecules is in the present work replaced by a model with both inertia and intrinsic moment of inertia. This extension introduces three rotational degrees of freedom into the dynamics of individual convective molecules, which enter into the dynamical equations for a mixing length fluid in the form of a separate vector field which we term the spin field. It is shown that for convective molecules having a spherically symmetric mass distribution the spin field is proportional to the local vorticity; the proportionality factor is termed the spin parameter.

The proposed dynamical equations for mixing length fluids contrast with conventional hydrodynamics in that the former contain anti-symmetric stresses and couple stresses, which according to Cauchy's second equation of motion and Cauchy's principle respectively vanish in conventional fluids. This difference is traced back to the non-central nature of the interaction between the spins of adjacent convective molecules.

Following the standard thermodynamic procedure, the transport equations for a mixing length fluid are derived from their dynamical equations for the simplest case that all transport coefficients are scalars. Because of the reversible nature of the motions of individual convective molecules the coefficients for the thermodynamical cross effects are subject to Onsager's reciprocity relations. For the solar convection zone an anisotropic viscosity and a latitude-dependent heat conductivity result, and the fluxes of heat and angular momentum are found to couple in a form that identifies the vorticity of the mixing length fluid as the vector potential of the convective heat flux. The coefficient characterizing this coupling, called the

thermomechanical effect, is different from zero only in the partially ion-
ized regions of the solar convection zone.

Because of the absence of sources or sinks of heat in the solar convec-
tion zone and its symmetry properties the convective heat flux can be re-
presented in a simple analytic form. The principle of minimum dissipation
for steady state dissipative processes is invoked to rule out azimuthal heat
fluxes. This is sufficient to obtain normal mode expansions for the azimu-
thal motions of the convection zone as a whole and for small cylindrical
sections of it. The meridional motions are represented analytically by the
azimuthal component of the vorticity and by the stream function. The latter
is found to be subject to a partial differential equation with such boundary
conditions as do not allow a stable solution for the meridional motions.

As regards the rotation pattern, the solar convection zone divides
into a fully ionized region with vanishing thermomechanical effect and a
partially ionized region with non-vanishing thermomechanical effect. The
former comprises the bottom 85% and its angular velocity has an inverse
cube dependence on distance from the center, and no latitude dependence;
the top 15% of the convective layers has both depth- and latitude-depen-
dence in the rotation rate in a way that matches the latitude-dependent
surface rotation and the latitude-independent rotation of the underlying
layers. The ensuing discontinuities of the radial angular velocity gradients at
the interfaces are matched by surface currents of mass and heat.

The Evershed flow and the supergranulation are interpreted as surface
manifestations of underlying vortex rings. The analytic forms for the azi-
muthal vorticity and the stream functions are derived, and the dependence
of the surface flow on distance from the symmetry axis is given. The struc-
ture of the flow pattern is illustrated with the streamlines and contour
lines of the velocity. The general properties of the flow resemble those
found in connection with cellular convection of conventional fluids.

ACKNOWLEDGMENTS

CONTENTS

LIST OF TABLES

LIST OF ILLUSTRATIONS

I INTRODUCTION

In the present chapter the problems with which this dissertation deals will be sketched in their historical perspective and modern significance, and the previous attempts at theoretical explanation will be discussed and contrasted with the approach which is adopted in the present work. The following discussion is meant to serve as a qualitative guideline for the more elaborate treatments in the subsequent chapters.

I.1 Statement of the Problem.

At the present time three types of steady mass motions on the sun are known. The longest known is the solar rotation, which has the peculiarity that on the solar surface the equatorial regions move more rapidly than the polar regions. The second type of steady mass motions is associated with sunspots throughout their existence; these motions are concentrated in the penumbral regions of spots. The most recently discovered steady motions cover the entire solar surface with a polygonal network of horizontal flow patterns; this is the supergranulation.

It is widely accepted that these steady flows on the solar surface are manifestations of motions in the underlying layers of the sun. Because of the inaccessability of these layers to direct observation, understanding of their characteristics must come from physical principles. This approach has met with considerable success insofar as the static properties of the sub-surface layers are concerned. In the matter of the structure of the flow patterns below the surface the situation is entirely different. Several aspects of these patterns remain even qualitatively unknown, the most glaring uncertainty being the sign of the radial gradient of the rotation rate below the surface. The failure to give a theoretical explanation for the observed mass motions stems from the incomplete understanding of the turbulent state which characterizes the top layers of the sun.

I.1.1 Historical Perspective.

The discovery of motion on the sun coincides with the introduction of the telescope into observational astronomy. Early in the 17th century Galileo pointed his telescope at the sun and found spots on the solar surface whose diurnal motions indicated a rotation rate "of about a lunar

month". Although a tendency for equatorial spots to have shorter rotation periods than spots situated at higher litutudes was noticed shortly afterwards by Scheiner, more than two hundred years passed before the full extent of this phenomenon was realized by Carrington, who put it on a firm and quantitative observational basis. From systematic observations of diurnal motions of sunspots the conclusion was inescapable that the sun does not rotate like a rigid body, but that on the solar surface the rotation rate is largest on the equator and decreases towards the poles. This phenomenon is known as the equatorial acceleration of the sun. The data on sunspot motions which have been collected in later years have amply confirmed Carrington's conclusions.

With the introduction of the high-resolution spectrograph at the beginning of the present century, it became possible to measure Doppler shifts due to rotation in a variety of spectral lines from the sun. This approach revealed not only differential rotation with respect to latitude, but also with respect to height in the solar atmosphere. The layers where the absorption lines of the Fraunhofer spectrum originate were found to rotate slower than the sunspots, whereas the lineshifts in the strong emission lines indicated a slightly higher rotation rate for the regions that they represent. These results have been confirmed and refined by modern spectroscopic investigations.

A new method of investigation of the surface rotation was provided by the spectroheliograph, which allows to take pictures of the solar surface in a narrow spectral region. In the light of Hα dark filaments are found on the solar disk which are the longest lived transient features of the sun. The rotation of a large collection of dark filaments was found by L. and M. d'Azambuja to closely follow the sunspot rotation rates. For determinations of the rotation rates the filaments have the advantage over sunspots that they extend to much higher latitudes. As a result, the analytic representation of the latitude dependent rotation rate of filaments goes to higher order than that for the sunspot rotation.

The most recent innovation in measuring the solar rotation is the use of the magnetograph in the Doppler mode. This instrument is especially suited for compiling vast amounts of data on a single spectral line for the entire surface of the sun. These measurements reveal the temporal structure

of the equatorial acceleration. The difference of the polar and equatorial rotation rates is found to fluctuate with an amplitude larger than the average value of this quantity. The unequaled capacity of the magneto-graph method for data acquisition and reduction seems likely to lead to the discovery of more new aspects of the surface rotation of the sun, for example the definite establishment of differences in rotation rate at equal latitudes on the northern and southern hemispheres.

By comparison with the solar rotation the other two types of steady motion on the solar surface take place on a much smaller scale. For the detection of the motions in sunspot penumbras a combination of good spatial and spectral resolution is required, whereas the supergranular motions border on present day instrumental detection limits.

Early in this century Evershed was trying to detect cyclic mass motions around sunspots which he expected there because of the recently discovered vertical magnetic fields in sunspot umbras. The penumbral line shifts which he detected surprised him by indicating a horizontal outflow from the umbra rather than the anticipated cyclic flow. The mass flows associated with all sunspots is now commonly called the Evershed flow.

All the spectroscopic techniques mentioned in connection with the rotation have been employed to investigate the detailed structure of the penumbral flow patterns. In this regard two major controversies remain. The first regards the extent of the flow into the unperturbed surrounding photosphere. Evershed always stuck to his original view that the lineshifts end abruptly at the outer boundary of the penumbra, but the second investi-gator, St. John at Mount Wilson, found that in his spectra the shifted lines returned gradually to their undisturbed positions. This controversy has persisted up to the present day, and is now connected with a second controversy regarding the precise location of the outflowing gases.

Under good seeing conditions the penumbra seen in white light resolves into bright penumbral filaments against a darker background. With a qualitative spectroheliogram method, Beckers found that the outflow takes place in the dark interfilamentary region, and stops abruptly at the outer penumbral boundary, whereas Schröter has concluded from time sequence pictures of sunspots obtained during the Stratoscope project that the mo-tions are confined to the bright penumbral filaments, and extend well into

3

the surrounding photosphere. Other investigators report the presence of faint satellite lines in the penumbra. To complicate the picture even more, the Evershed effect has recently been reinterpreted by Maltby not as a Doppler shift but rather as a strong line asymmetry due to wave motions in the penumbra.

The discovery of the supergranular network followed shortly after a refinement of the spectroheliograph technique was introduced by Leighton. The new technique allowed to filter out certain oscillatory components of the velocity field by photographically subtracting spectroheliograms taken at suitable time intervals. In this way a higher spatial and spectral resolution can be obtained than with the other spectroscopic methods. This is necessary because the velocities associated with the supergranulation are about an order of magnitude lower than typical Evershed velocities. Also the flow is less steady than the penumbral outflow. The supergranular lifetime is about an order of magnitude shorter than that of a typical sunspot of comparable size.

I.1.2 Modern Significance.

All three types of steady mass flows discussed in the previous section are thought to have far reaching effects on many aspects of the behavior of the sun and on solar-terrestrial relationships. Foremost among these is the 11 year cycle in solar activity which is responsible for a host of geomagnetic phenomena ranging from aurorae to disturbances of the ionosphere which hamper radio communications.

In the modern magnetohydrodynamic theory of the solar cycle by Babcock (1961) a weak poloidal magnetic field in combination with differential rotation below the solar surface gives rise to gradually increasing toroidal fields which become buoyant and break through the solar surface to form sunspots and active regions. In Leighton's (1969) more elaborate version of this theory, the supergranular motions then gradually erode the sunspot fields and disperse them by a random walk process over the entire solar surface in such a way that the original poloidal magnetic field is reversed. The cycle then recommences with opposite magnetic polarities.

It is clear that in this model the subsurface rotation pattern has decisive influence on the structure of the toroidal magnetic fields which build up below the surface during the field amplification phase. The theory

4

requires for its satisfactory operation an inwardly increasing angular velocity gradient and concentration of shear below the equatorial regions of the sun. Of equal importance for the field eruption phase of the model is the supergranular flow. In this case the interest focusses not so much on the detailed flow pattern as on the average size and lifetime of individual supergranules since these parameters will determine the efficiency of the random walk process. Finally the penumbral flows may be expected to play an important role in the problem of the evolution of individual sunspots and active regions. It is fair to say that the mass flows on and below the solar surface determine in good measure the nature and complexion of the many phenomena which are connected with the solar cycle.

A second area where mass motions may have important as yet unknown effects lies in the field of stellar evolution. The rotational history of average stars like the sun is presently the subject of a widespread controversy, the main issue being the present rotation rate of the central solar regions. The subject also has important ramifications for the early evolution stages of the sun in connection with the formation of double stars and of planetary systems. During the later evolutionary stages there is the further problem of the observed correlation between the spectral type and the surface rotation of main sequence stars. A comprehensive theory of stellar rotation, possibly in combination with meridional motions, should shed light on all of the above problems.

Lastly the present interior rotation of the sun could have cosmological implications. If the central regions of the sun rotate at more than ten times the surface rate, the resulting gravitational quadrupole moment would alter the perihelion advance of Mercury to an extent that would destroy the present good agreement with the value calculated from Einstein's theory of general relativity.

I.2 Previous Attempts.

The basic difficulty standing in the way of a theoretical treatment of the fluid motions on and below the solar surface is the turbulent state of the sub-surface layers. This was realized already in the previous century when the granular appearance of the solar surface in white light was discovered. The turbulent motions are a result of the convective heat transfer from the hot solar interior to the cooler surface layers. For

the description of such thermal turbulence, an approximate theory has now been developed to a level where quantitative profiles for the pressure, temperature, density and several other variables for a convection zone can be obtained. This is the mixing length theory, which plays a vital role in the current understanding of stellar convective envelopes and of stellar structure and evolution in general.

The ideas contained in the mixing length theory also form the starting point of investigations concerning the effect of rotation on turbulent convection. An early attempt in this direction led to the view that a spinning convective envelope would not rotate like a rigid body, but would in the steady state, be characterized by a non-uniform angular velocity distribution. This result cannot be obtained within the framework of conventional hydrodynamics. Most theoretical work on the rotation of convective envelopes has concentrated on the effects of modifying the transport coefficients such as viscosity and heat conductivity in a way consistent with the mixing length theory. In this way the rotation pattern can be brought in basic agreement with the latitude-dependent differential rotation observed on the solar surface.

With regard to the small-scale mass motions on the solar surface, the situation is essentially different in that these presumably are independent of the rotation. A non-rotating sun would be similarly covered with a super-granular network, and any occurring sunspots would have Evershed flow in the penumbral regions. The cause for this type of flow is generally sought within the framework of conventional hydrodynamics, because of the existing laboratory experiments on cellular convection and the successful theoretical description thereof. These experiments certainly reveal superficial simi-larities between cellular convection in the laboratory and on the sun, but a full account for the mechanism responsible for the solar motions is as yet lacking.

I.2.1 Anisotropic Viscosity.

In 1946 Wasiutynski introduced the idea that in convection zones the turbulent momentum exchange should be anisotropic because of the preferred direction which gravity establishes for the convective motions. This idea was formalized by replacing the usual scalar viscosity coefficient in the Navier-Stokes equations by a diagonal viscosity tensor, in which the ratio

of the vertical component to the two horizontal components expressed the degree of anisotropy.

Soon afterwards, Biermann drew the consequences of Wasiutynski's views as applied to a model of mixing length convection in which the convective elements are treated as point masses subject to Coriolis forces. Without actually solving the modified Navier-Stokes equations, Biermann concluded from a kinetic discussion that the angular velocity in rotating convective envelopes should have a power law dependence on the radius, with the exponents lying between zero (for isotropic turbulence) and minus two (for purely monotropic turbulence in radial directions). This picture is preserved when convective angular momentum transfer by large scale meridional motions is included.

The modified Navier-Stokes equations proposed by Wasiutynski were solved by Kippenhahn with an approximation method valid for the case that viscous forces dominate over inertial forces. The inner and outer boundaries of the convective envelope were both assumed to be free surfaces, in order to reflect the discontinuous change in viscosity which occurs on the interface of a convective and a non-convective region. For the zero-order solution of his approximation method Kippenhahn recovered Biermann's rotation patterns, but for higher order the method failed to converge. On the real sun inertial forces cannot be neglected compared to viscous forces in the convective layers.

A second attempt to solve Wasiutynski's equation was made by Sakurai employing a different approach. Sakurai adopted Kippenhahn's boundary conditions, but used as the expansion parameter the relative thickness of the convective shell. After heroic calculations, a complicated explicit dependence of the rotation pattern on the anisotropy parameter resulted. For enhanced momentum transfer in radial directions, a meridional circulation rising at the poles and sinking at the equator was found, and the rotation pattern exhibited equatorial acceleration combined with an inward decrease of angular velocity, whereas for reduced radial viscosity the results were opposite.

Recently direct numerical solutions of the modified Navier-Stokes equation have been published by Köhler. The boundary conditions are the same as with the previous authors, and the validity of these conditions with regard to the solar wind torque are verified. The results confirm the general picture which had evolved from the earlier analytical work.

7

I.2.2 Latitude-Dependent Heat Conductivity.

The purely hydrodynamical approach to the solar mass motions is necessarily incomplete in that no information about the temperature distribution and the heat flux is obtained. The reason for this is that for the equation of state of the mixing length fluid, the adiabatic relation between pressure and density has been assumed. In that case the continuity equation and the Navier-Stokes equation form a determinate set leading to barotropic flow patterns for given geometries and boundary conditions. In a more general approach the temperature field can be introduced into the force balance by replacing the barotropic equation of state by the ideal gas law. It is then necessary to include the energy balance of the fluid to obtain again a determinate system. This is termed the baroclinic approach, because in this case the surfaces of constant pressure and constant density no longer need coincide.

From laboratory experiments on the effect of rotation on convection one expects that the rotation of the sun would interfere with its convective heat transfer. The effect would be different at the equator, where the directions of gravity and rotation are perpendicular, and at the poles, where the directions of gravity and rotation are parallel. Accordingly, the poles and the equator would have different outward convective heat fluxes, which would result in temperature differences between the polar and the equatorial regions of the sun. In such a baroclinic situation, thermally driven meridional motions would be generated in order to offset the polar-equatorial temperature difference. This could again result in equatorial acceleration, as with the mechanically driven meridional circulation in the barotropic case. The above line of thinking has been formalized in a recent paper by Durney and Roxburgh, in which a latitude-dependent heat conductivity is introduced in the conventional balance equations for mass, momentum and energy. Although with numerical methods the observed equatorial acceleration of the sun can be recovered, the solution also leads to a polar-equatorial temperature difference much larger than is actually observed on the sun and the solution fails to provide the dependence of the angular velocity on radius. Although broader in scope, the baroclinic approach has thus far yielded less than the more restricted baroclinic methods of the previous section.

I.3 Cellular Convection.

The granulated structure observed on the solar surface shows an overall

8

resemblance to the cellular convective patterns which Benard observed early in this century in thin layers of fluid heated from below. Such layers settle down in a regular pattern of equal sized hexagonal cells. The flow at the surface is away from the center and towards the boundaries with the other cells.

In formulating the Benard problem in hydrodynamical terms, Rayleigh used the Boussinesq-approximation, which neglects density variations, except in connection with the gravitational term in the force equation. The Boussinesq fluid is thus subject to buoyancy forces, but is at the same time kinematically incompressible. For the boundary conditions, Rayleigh assumed free surfaces and uniform temperatures on both sides of the fluid layer.

For the solution of the resulting perturbation equations, Rayleigh used a normal mode expansion satisfying the boundary conditions and dividing the layer in rectangular cells. In this way he was able to find a stability criterion for the onset of cellular convection, and also the resulting flow patterns inside individual cells. Subsequently, a great deal of work along the same lines was done for different geometries and boundary conditions. Also the effects of rotation and magnetic field on the onset of stability have been extensively studied. Many results of theory and experiments have been brought together in Chandrasekhar's monumental work on these subjects.

The similarities of laboratory and solar cellular convection suggest that the latter also fall in the realm of conventional hydrodynamics. Moreover, Rayleigh's instability criterion is satisfied in the solar layers below the surface and the Boussinesq approximation appears reasonable. In this manner, Davies-Jones and Gilman have recently obtained solutions in qualitative agreement with several solar phenomena connected with convection.

One important qualification must be made regarding the explanation of local solar motions as surface manifestations of Benard-type cellular convection. Whereas the Benard-cells settle down into a strictly steady state, the supergranulation remains a non-steady phenomenon with new cells appearing and old cells disappearing continuously.

I.4   The Present Approach .

In common with the earlier attempts, the starting point of our approach is the mixing length theory of turbulent convection, which describes a

convective layer as an ensemble of convective molecules with a given mean free path called the mixing length. However, regarding the kinetic behavior of the convective molecules, we make a different assumption than was introduced by Biermann. Our model for the convective molecules is not that of a point mass, but rather that of an extended mass distribution with a non-vanishing moment of inertia about its own center of mass. Moreover, we assume that the volume of this mass distribution may change during the lifetime of a convective molecule and that the moment of inertia will change with it. In the framework of the mixing length theory, such volume changes should occur in convective molecules undergoing vertical displacements in highly stratified convection zones like those found on stars.

I.4.1 Vorticity and Spin.

If the convection zone under consideration has an overall rotation each individual convective molecule will have in addition to its linear momentum also a non-vanishing angular momentum. The angular momentum will consist of two parts, namely the orbital angular momentum due to its rotation about the rotation axis, and the intrinsic angular momentum or spin due to the rotation about its own center of mass. In Biermann's point mass model for convective molecules there is no contribution to the total angular momentum from the spin because of the vanishing moment of inertia of a point mass.

A convective molecule moving freely in a rotating coordinate frame will in general experience a sideward Coriolis force on its center of mass which will curve its trajectory. If at the same time internal mass motions modify the moment of inertia of the convective molecule then this molecule will also be subject to a Coriolis couple which will change its intrinsic rotation rate.

In the mixing length picture convective molecules are formed in a fluid, travel over a distance of one mixing length and then dissolve again. If the convective region has an overall rotation then by the above-described mechanism the initial intrinsic rotation rate of a convective molecule will in general be different from its final intrinsic rotation rate. In this manner, the proposed process will introduce differential rotation in an originally uniformly rotating convective layer. The same qualitative conclusion was reached by Biermann in his discussion of his point mass model

10

of convective molecules. Our inclusion of moment of inertia essentially adds three rotational degrees of freedom to individual convective molecules. The implications of these degrees of freedom for the mixing-length fluid as a whole are considered next.

In order to quantify and formalize our approach a geometrical model for the volume changes of convective molecules during their lifetime has to be adopted. Any tractable model will necessarily introduce further idealizations of the real convective situation than are already inherent in the mixing-length picture. In such cases, it will be our policy to adopt the simplest possible formal expression of the proposed idea. For the present question of the changing geometry of a convective molecule, the simplest model is that of a spherically symmetric mass distribution undergoing uniform contraction or expansion. This "expanding sphere" model for convective molecules underlies our formulation of the dynamical equations for mixing length fluids just as Biermann's point mass model underlies the earlier formulation of these equations as Navier-Stokes equations with an anisotropic viscosity.

The "expanding sphere" model reduces the three rotational degrees of freedom associated with individual convective parcels to a single one for the mixing length fluid as a whole. Namely, for spherically symmetric volume changes the spin vector changes only in magnitude, but not in direction. With the initial intrinsic rotation rate of a convective molecule determined by the local vorticity of the mixing-length fluid, the subsequent changes in the intrinsic rotation rate can be described with a scalar proportionality factor to the local vorticity. In the continuum picture for the mixing-length fluid as a whole, the internal rotations can then be represented by a separate vector field equal in direction but unequal in magnitude to the vorticity field. We term this field the spin field, and its proportionality factor with the vorticity field will be termed the spin parameter.

The above considerations on how to describe the rotational state of a mixing length fluid call to mind the way in which the electric and magnetic properties of materials are described. In each of these cases there are two different vector fields necessary to describe the electric resp. magnetic state of the material, and in each case the two vector fields are for many materials connected by a scalar proportionality factor. One immediate consequence of the two-field representation is the existence of surface charges

11

and surface currents in electric and magnetic materials respectively. A further consequence of a thermodynamic nature are the various thermoelectric and thermomagnetic phenomena occurring in electric and magnetic materials subject to temperature gradients and heat fluxes. The formulation and properties of these thermodynamic cross-effects suggest that analogous relations exist between the heat flux and the rotational state of a mixing-length fluid.

I.4.2 Thermomechanical Effect.

The derivation of the thermodynamic cross effects in general follows in a rigorous manner from the second law of thermodyhamics. For the present case of a fluid possessing spin, the dynamical equations have to be formulated in order that the entropy balance can be found. What will be the dynamical effect of the fluid properties embodied in the spinfield? We propose that in such a fluid, the stresses not only tend to displace, but also tend to rotate surface elements. In other words, couple stresses as well as ordinary stresses should be significant in the rotating mixing length fluid. This constitutes a second break with conventional hydrodynamics, in which the neglect of couple stresses is known as Cauchy's principle. The underlying difference between conventional fluids and mixing length fluids is that ordinary molecules will generally interact with each other through central forces, whereas the spin interactions of convective molecules will in general have a non-central character.

The standard thermodynamical procedure for deriving linear transport equations from the dynamical equations leads for a fluid possessing spin to modifications of the conventional equations for viscous momentum transfer and conductive energy transfer. These modifications are in harmony with the changes which previous authors have introduced in order to describe the rotational state of the solar convection zone. The proposed spin parameter can be identified with the parameter representing the anisotropy of the viscous forces which underlies the barotropic treatment of mixing length fluids. In the baroclinic treatment the effective heat conductivity is found to have two components with complementary latitude dependencies.

From a physical point of view, the essential implication of the spin field is that in rotating mixing length fluid there can be two different modes of energy transfer, which arise respectively from the translational and the rotational motions of convective molecules. At the same time these

12

motions bring about transfer of angular momentum, with the net result that in rotating mixing length fluids the fluxes of heat and angular momentum are coupled. The above-mentioned thermodynamic procedure provides an exact formulation of this coupling. In the simplest case of an isotropic fluid the coupling is expressed by a scalar coefficient called the thermo-mechanical effect.

The view that the effect of the temperature field on the angular momentum flux and of the spinfield on the heat flux can be represented by a single scalar coefficient derives from Onsagers reciprocity relations for coupled dissipative processes. For these relations to be valid, the microscopic equations of motion for the elementary constituents involved have to be time-reversable. In the mixing length theory the elementary constituents are the convective molecules. The equation of motion for indi-vidual convective molecules balances their inertia with their buoyancy, to the exclusion of any dissipative forces. Thus the equations of motion for individual convective molecules as well as ordinary molecules are time-symmetric, and with regard to the properties of large ensembles of each of them the same conclusions may be drawn.

The reversable nature of the motions of convective molecules has a direct consequence on the amount of work that each of them can do on its environ-ment. In the translational mode each convective molecule can be imagined as performing a thermodynamic cycle between two heat reservoirs at different temperatures. In the mixing length picture of convective heat transfer, the branches of this cycle are two adiabatics representing the vertical motions, and two isobarics, representing the subsequent thermalization of the convective molecule with its environment. A similar cycle will repre-sent the rotational mode. In both cases, the convective molecule acts as a reversible thermodynamic engine, whose efficiency, according to Carnot's principle, is determined completely by the temperatures of the two heat reservoirs between which the engine operates. In this manner up to 95% of the energy traversing the solar convection zone could in principle be converted into work. In practice, the work done by convective molecules in the translational mode will be randomized rapidly into large-scale turbulent motions; the work done by convective molecules in the rotational mode can lead to ordered flow patterns if an external or internal ordering agency is at work in the fluid. An example of such an ordering agency are the Coriolis couples which in the earlier discussion made the spins of

13

convective molecules parallel to, but slightly different in magnitude from the local vorticity.

We now turn to the question what relevance our approach may have to the local mass motions which are in evidence on the solar surface. It is clear that these motions are not connected in any essential way with the solar rotation. From a physical point of view, the question then is whether in the absence of external rotation still a rotational mode of heat transfer can develop. A consideration of the rotational stability of a convective molecule in a super-adiabatic fluid layer answers this question in the affirmative. The procedure is essentially the same as for deriving the Schwarzschild criterion for translational instability, except that an adiabatic vertical displacement is now replaced by an adiabatic rotation about a horizontal axis. In the one case, the resulting buoyancy force tends to displace the convective molecule further, in the other the resulting buoyancy couple tends to rotate it further. In fluids with a super-adiabatic temperature gradient, the generation of rotational as well as translational turbulent energy will occur.

For the fluid as a whole the above-described rotational instability leads to a volume distribution of mass circulations on the molecular level. This picture affords a justification of the analytic form of the rotational heat flux as well as a physical interpretation of the thermomechanical effect in terms of the microscopic properties of the fluid. Beginning with the latter, we note that convection zones will generally consist of gases which are fully or partially ionized. In the first case, the internal energy of the gas depends only on pressure, in the second it depends beside the pressure on other thermodynamic parameters. For this reason, no energy transfer is associated with a pure rotation of a fully ionized convective molecule, whereas the circulation of a partially ionized convective molecule will be accompanied by a current loop of heat. Along these lines a significant rotational heat flux will only be expected in layers with significant partial ionization, as is the case in the regions immediately below the solar surface.

The identification of volume distribution of current loops of mass and heat further illustrates the analogies which our description of the rotational state of a mixing length fluid has with the classical description

of magnetic materials. In terms of this analogy, these circulations correspond to the microscopic electric currents which according to Ampere's hypothesis underlie all macroscopic magnetic phenomena. In keeping with this analogy, our description of rotating mixing length fluids will comprise discontinuities of the vorticity and spinfields at the boundaries of convective regions, and surface currents of mass and heat matching these discontinuities. Each of these unorthodox aspects of the present theory will be seen to account for some of the more bewildering observational aspects of the mass motions occurring in the convection zone of the sun.

15

II STRUCTURE OF THE SOLAR SURFACE

In the present chapter the available observational data on solar structure, energy flux and mass flow will be employed to arrive at simple models for each of these. As regards the spatial structure of the sun, we distinguish between the global level for observations pertaining to the sun as a whole, and the local level for observations pertaining to small regions of the sun. The length scale of the local level is such that the curvature of the solar surface can be neglected. This criterion brings sunspots and individual supergranules in the class of local phenomena.

As regards the time-structure of solar characteristics, we will distinguish between steady, transient and periodic phenomena. The steady characteristics comprise those which have not changed measurably since systematic observation of the sun began; examples are the solar radius and luminosity. Transient phenomena are those whose beginning and end can be observed; sunspots and supergranules fall in this category. The most striking periodic phenomenon of the sun is the 11-year cycle in solar activity which affects a wide range of solar and terrestrial phenomena. The above categories are established here with a view on the theory of convective heat transfer which will be developed in Chapter IV.

The instruments and techniques used in studying the morphology of the solar surface are scarcely less numerous than the problems that present themselves. The oldest instrument, the telescope, has now been developed to a point where the atmospheric refraction is the major obstacle to improved spatial resolution. The present limit is about 1 arcsec, or 700 km on the sun. With modern spectrographs the Doppler effect in spectral lines from the sun can be measured down to velocities of about 100 m/sec. Various optical and photographic techniques reveal the two-dimensional structure of magnetic and velocity fields with an accuracy approaching the above limits. Especially in the matter of the fine structure of the various velocity fields on the sun, there still is considerable difference of

opinion among the different observers. The following presentation of observational material aims at illustrating generally accepted features of the mass flows on the solar surface. Controversial viewpoints are included only when the solutions given in Chapters V and VI seem to clarify them.

II.1 Global Structure.

In white light the sun presents itself as a circular disk whose brightness decreases with distance from the center. At the limb the brightness drops abruptly to a tiny fraction of the surface value. This sharp transition provides the operational definition for the solar radius.

The latitude-independent decrease of brightness away from the center of the disk is known as the limb darkening. This phenomenon demonstrates that the observed characteristics of the solar surface depend on the angle under which they are observed. This observational effect must be accounted for before the physical properties of two different regions of the sun can be compared. In practice all regions of the sun can be observed under different angles because of the solar rotation. In assigning a radius or an effective temperature to the solar surface it will always be understood that the observations have been reduced to the same observation angle. For the measurements of the radius and temperature the line of sight will be respectively tangential and normal to the solar surface.

II.1.1 Dimensions.

The recognition that the sun has a spherical shape dates back to antiquity. With modern photometric methods the radius of the white-light emitting layers of the sun can be found in five significant figures (Allen, 1963), giving:

$$R_\odot = 6.9598 \times 10^5 \text{ km} \tag{1}$$

This leaves an uncertainty in the average solar radius of about 10 km.

Because of the centrifugal force, the rotation of the sun as observed on the surface will cause a difference in polar and equatorial radii of

17

about 7 km. The actual magnitude of the oblateness of the photospheric layers is at the present time controversial. A value five times larger than consistent with the surface rotation has been reported (Dicke, 1970). For this measurement several explanations other than a rapidly rotating interior have been proposed, such as radial differential rotation (Roxburgh, 1967), meridional circulation (Cocke, 1967) or magnetic fields (Sturrock and Gilvarry, 1967). With modern techniques no time variation has been found in connection with the solar cycle.

II.1.2 Energy Flux.

The bulk of the solar energy output is emitted in the visible part of the electromagnetic spectrum. As witnessed by the uniform temperature of the emitting layers, the energy flux is evenly distributed over the solar surface. There is no systematic temperature difference detectable between any two points of the photosphere. This holds over time scales long compared with those of the transient phenomena of sunspots, granulation, etc. The total radiative output of the sun, the solar luminosity, is also found time-independent. There is no correlation with the phase of the solar cycle.

The absolute value of the solar luminosity cannot be determined as accurately as the solar radius, mainly because of the unknown absorption of intervening gases. The most accurate bolometric observations (Allen, 1963) give:

$$L_{\odot} = 3.90 \times 10^{33} \text{ erg/sec} \tag{2}$$

In the remainder of this work the above figure is adopted as representing the entire energy output of the sun.

II.1.3 Mass Motion.

The global mass motions in evidence on the solar surface represent a rotation. The nature of this rotation is not that of a rigid body. The regions near the equator have higher rotation rates than the polar regions; this is termed the equatorial acceleration of the sun. Layers at different heights also display differences in rotation rate. The observed rotation

rates show strong fluctuations with time. In addition to the rotation there is also some evidence for global meridional motions on the solar surface.

II.1.3.1 Rotation.

The rotation of the sun was first inferred by Galileo from his observations of the diurnal motions of sunspots. From systematic observations of sunspot motions the latitude dependence of the surface rotation rate was discovered (Carrington, 1863). These conclusions were confirmed by similar measurements on other identifiable features of the solar surface with a long enough lifetime, and from spectroscopic measurements on a large number of spectral lines. The latter also have borne out the strong height dependence of the rotation rate of the photospheric layers.

II.1.3.1.1 Orientation of the Rotation Axis.

From the paths of markers across the solar disk or from spectroscopic measurements, it is found that the rotation axis of the sun is inclined with respect to the plane of the ecliptic at an angle of about $7°10'$. The orientation of the rotation axis does not seem to change with time (de Lury, 1939). Looking down on the north pole of the sun, the rotation is anti-clockwise. The period of rotation with respect to the earth is termed the synodic period. Because of the uneven orbital motion of the earth, this period varies in the course of the year. In the present work we will consistently employ rotation periods corrected for the earth's orbital motion. This rotation period with respect to the fixed stars is termed the sidereal period of rotation.

For analytical purposes we will use a right-handed Cartesian coordinate frame with spherical coordinates. The origin of this frame lies at the center of the sun and the polar axis lies along the axis of rotation with the positive direction pointing north. The coordinate frame is at rest with respect to the fixed stars.

II.1.3.1.2 Latitude Dependence.

All methods employed for measuring the latitude dependence of the angular velocity in the observable layers of the sun display large fluctuations

between individual data points. Such fluctuations frequently exceed the average value of the equatorial acceleration. Only after averaging over large data sets does a regular pattern emerge. Two extreme types of data sets are provided by the sunspots and the magnetograph measurements in the Doppler mode. The sunspot data form a homogeneous set covering more than a century. This includes several solar cycles. The magnetograph method provides a large amount of data in a short period of time. Although systematic magnetograph measurements have been initiated only recently, they provide far and away the most accurate measurements on the spatial structure of the equatorial acceleration.

II.1.3.1.2.1 Geometric Method.

The systematic observation of sunspot motions which originally revealed the solar rotation and its latitude dependence now covers a period of more than a century. During this period there is no evidence for a systematic change in the rotation pattern (Newton and Nunn, 1951). Although the rotation rates of individual spots may deviate considerably from the average value for their latitude, the average rotation rate does not vary appreciably with the phase of the solar cycle or from one cycle to another. This makes the equatorial acceleration a steady phenomenon in the sense defined earlier. Since sunspots are generally confined to the region within 35° of the solar equator, the rotation pattern at higher latitudes must be inferred from other methods.

The longest lived transient phenomena on the solar surface are the dark filaments which appear in Hα-pictures of the solar disk. On the limb they appear as bright quiescent prominences. With these the surface rotation may be determined up to latitudes of 70° (d'Azambuja, L. and M., 1946). The results are in essential agreement with the sunspot measurements.

II.1.3.1.2.2 Spectroscopic Method.

In the spectroscopic method the Doppler shift of individual spectral lines is measured. This method qualitatively confirms the latitude dependence and steadiness of the surface rotation as found with the geometrical method. Quantitatively, the spectroscopic data are quite inhomogeneous.

In the photospheric absorption lines the rotation rate is below that of the underlying convection zone. This applies to all latitudes. In the chromospheric and coronal emission lines a latitude dependence is found which generally follows that of the underlying solar surface (Allen, 1963).

The use of the magnetograph has revealed several new aspects of the surface rotation (Howard & Harvey, 1969). When measured on a day-to-day basis, the equatorial acceleration is found to have fluctuations exceeding the average value of the polar-equatorial difference in rotation rate. As a whole, the magnetograph data demonstrate the presence of a systematic difference in rotation rates at the same latitudes on the northern and the southern hemispheres. A third result of the magnetograph data is that the weak photospheric magnetic field displays a smaller latitude dependence in the rotation rate than found from spots and prominences (Wilcox and Howard, 1970). At low latitudes the photospheric magnetic field lags behind the surface rotation, at high latitudes above 30° it rotates faster than the surface. The magnetograph data represent the most accurate measurements to date, because the number of data points contained in them exceeds that of the geometric or spectroscopic data by several orders of magnitude.

II.1.3.1.3 Radial Dependence .

In the order of increasing distance from the center the solar layers whose rotation can be measured directly are the top of the convection zone, the photosphere, the chromosphere and the corona. The markers for each of these layers are respectively the sunspots and prominences, the absorption lines and the emission lines. Going upward from the top of the convection zone the rotation rate appears to suffer a discontinuity at the interface with the photosphere. At any given latitude the lowest rotation rate is found in the weakest photospheric lines representing the deepest layers of the photosphere (Solonsky, 1972). With increasing height the rotation rate rapidly increases to a value comparable to the surface rotation. At the level of the first emission lines the rotation rate tends to follow the rotation rate of the surface directly underneath. This tendency persists into the coronal layers, where the rotation pattern found in the K-line closely follows the latitude dependence found for the dark filaments (Allen, 1963).
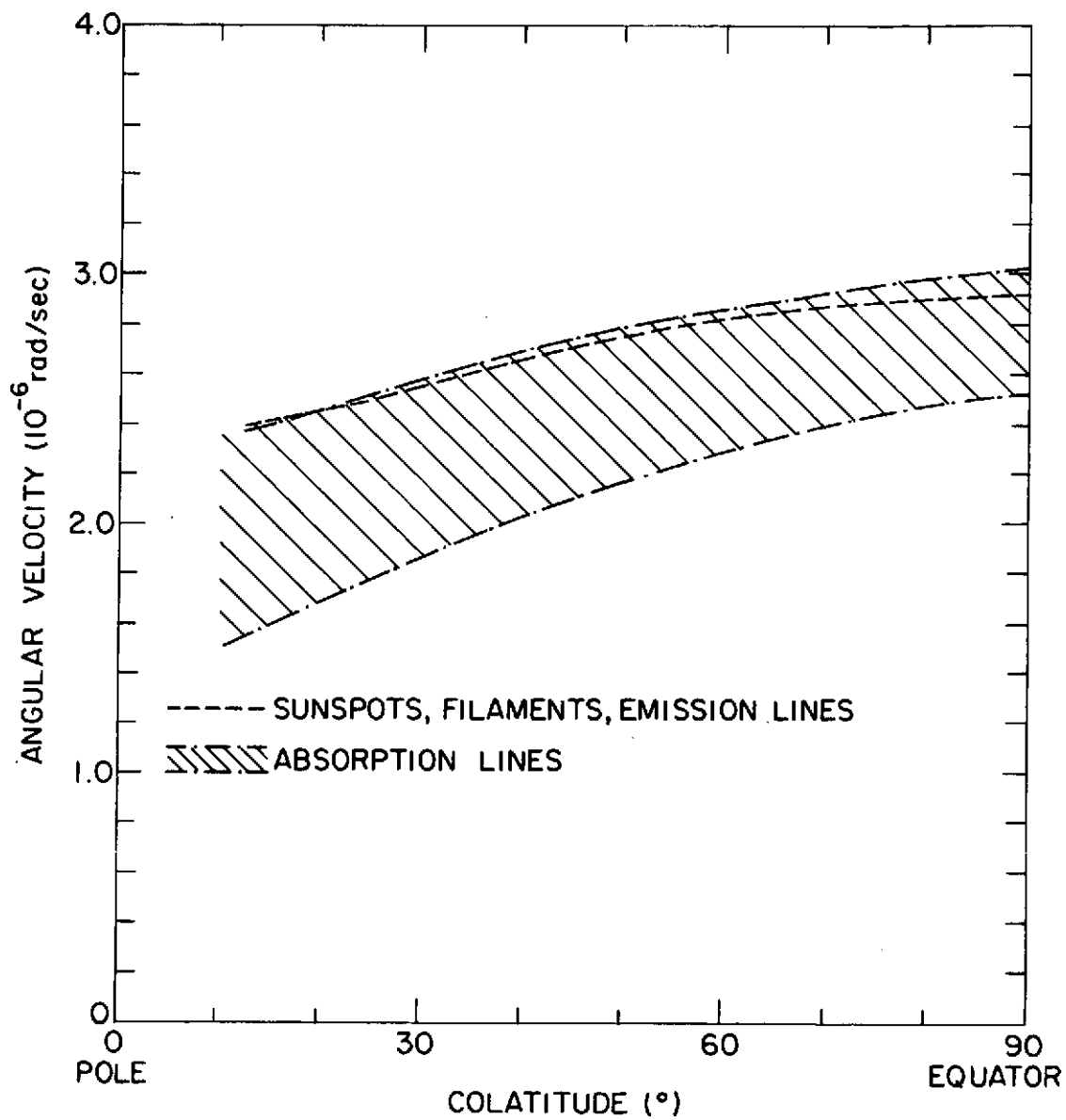
Figure 1. Observed latitude dependence of the
angular velocity of the solar material.
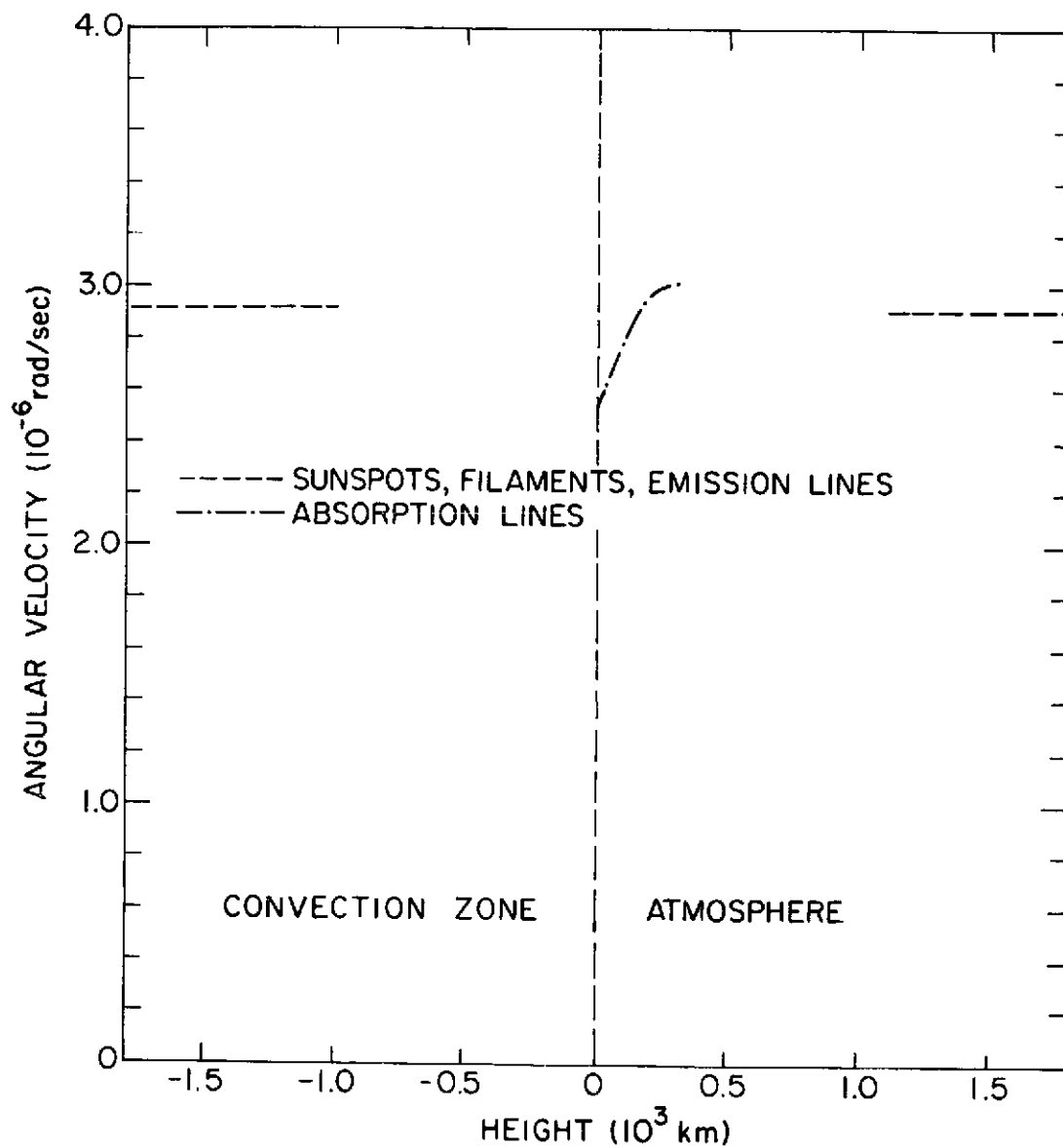
Figure 2. Observed height dependence of the angular velocity of the solar material at the equator.

In contradiction with the above idealized picture of the rotation of the observable layers of the sun, the rotation rate in Hα has been reported as faster than that of the magnetic structures embedded in the convection zone (Livingston, 1969). The same author finds no height dependence in the rotation rate of the photospheric layers.

II.1.3.1.4 Model.

In order to represent the observational data in analytical form the latitude dependent angular velocity is commonly expressed as a power series in the sine of the latitude, or, equivalently, the cosine of the colatitude. The even terms of this expansion express differences between the polar and equatorial rotation rates, and the odd terms express any differences in rotation rate between the two hemispheres. The coefficients of the series expansion are different for different levels of the solar layers. With Ω denoting the orbital angular velocity and θ the colatitude we have:

$$\Omega = \sum_{n=0}^{\infty} \Omega_n \cos^n \theta \qquad (3a)$$

$$\Omega(\frac{rad}{sec}) = \frac{\Omega(\frac{rad}{yr})}{3.17 \times 10^7} = \frac{\Omega(\frac{deg}{day})}{4.95 \times 10^6} = \frac{7.27 \times 10^{-5}}{T(days)} = \frac{v(\frac{km}{sec})}{6.96 \times 10^5} \qquad (3b)$$

Equation (3b) connects the various forms in which numerical values for the rotation are given in the literature. According to Equation (3a) the equatorial rotation rate is given by Ω_0. For solar layers whose rotation has been given in the form (3a) the non-vanishing expansion coefficients are given in Table 1.

The most recent spectroscopic observations on the photospheric rotation are not available in the form of the coefficients of Equation (3a) (Solonsky, 1972). These have been represented graphically in Figure 1 depicting the latitude dependence and Figure 2 depicting the radial dependence of the angular velocity of the observable solar layers.

Table 1

OBSERVED VALUES FOR THE EXPANSION COEFFICIENTS OF
EQUATION (3a) FOR DIFFERENT MARKERS ON THE SUN

Marker	Period	Range of $\|\pi/2-\theta\|$	$\Omega_0(10^{-6} \frac{rad}{sec})$	Ω_2/Ω_0	Ω_4/Ω_0
Sunspots	1878-1944	35°	2.90	-.193	
Filaments	Before 1946	70°	2.91	-.097	-.092
Feλ5250	1966-1969	85°	2.78	-.126	-.159

We adopt the following model for the rotation pattern of the observable layers based on the above mentioned observations.

(i) The top layers of the convection zone have a latitude dependent rotation rate. The average value of this rotation rate is best represented by the results derived from filaments.

(ii) The bottom of the photosphere has a rotation rate which at all latitudes is substantially slower than that of the underlying convective layers. With increasing height the photospheric rotation rate increases rapidly to reach at its top a value close to that of the underlying convective layers.

(iii) The chromosphere and corona have the same rotation rate as the convective layers below them.

The rotation pattern described above is illustrated in Figures 1 and 2 depicting the dependence on latitude and on height of the rotation rate encountered in the observable layers of the sun.

In addition to the quantitative and well-accepted knowledge of the solar rotation summarized above there is a wide variety of observations pertaining to the interior rotation of the sun. These observations are necessarily of a more indirect character, and for the most part they only give qualitative indications on the rotation pattern below the surface. The specific goal of many of these measurements is the determination of the radial angular velocity gradient below the surface. At the present time it is not

known whether the angular velocity decreases or increases with depth below the surface. We will now review several attempts at measuring this quantity.

It is observed that more sunspots are born on the approaching than on the receding hemisphere of the sun (Maunder, 1907). This east-west symmetry has been ascribed to a forward tilt of the sunspot axis due to a decrease of rotation rate below the surface. The tilt is found to increase with the lifetime of the spot (Minnaert, 1946). Quantitatively, the required radial shear is about an order of magnitude lower than the largest observed latitudinal shear (Piddington, 1972).

A second indication that in the sunspot region the rotation rate decreases inward comes from the observed helicities of chromospheric whirls (Hale, 1927) and from polarization effects in sunspots (Bumba, 1962). These observations show that magnetic flux tubes on the sun may be twisted in either sense. If the twisting is to be due to the differential rotation of the convective layers then again an inward decrease in rotation rate in the sunspot region is indicated (Leighton, 1969; Piddington, 1972).

The rotation of the central regions of the sun has been investigated through its effect on the oblateness of the solar surface. The observed oblateness was found to be five times larger than could be caused by the centrifugal force stemming from the surface rotation. The reported value would require a core measuring half a solar radius to have a rotation period of two days (Dicke, 1970).

II.1.3.2 Meridional Circulation.

By comparison with the azimuthal motions described earlier, the systematic motions of the solar surface in meridional planes turn out to be very slow. On the average, sunspots below and above 20° latitude move towards and away from the equator respectively (Richardson and Schwarzschild, 1953; Tuominen, 1956). There also is a poleward migration of polar prominences associated with the solar cycle (Ananthakrishnan, 1954; de Jager, 1959).

II.2 Local Structure .

In the introduction to this chapter the local level was defined as
the level on which the curvature of the solar surface can be neglected.
For definiteness the maximum length scale of the local phenomena is taken
as an order of magnitude less than the radius of curvature of the solar
surface, or 70,000 km. With this criterion even the largest individual
sunspots will fall in the category of local phenomena and the same will
hold for individual supergranules with their 32,000 km diameter.

The study of local phenomena requires a higher spatial resolution than
is necessary for studies of the solar surface as a whole. The best avail-
able instruments now achieve a spatial resolution of 1 arcsec, or 700 km on
the sun. This allows an accurate determination of the dimensions and energy
fluxes of the local phenomena. As regards the local mass motions, the com-
bined requirements of high spatial and spectral resolution stand in the way
of a precise determination of the flow patterns. In particular the struc-
ture of the flow in sunspot penumbras remains the subject of several long-
standing controversies.

For the description of the local phenomena it is convenient to intro-
duce a Cartesian coordinate frame with cylindrical coordinates ρ, φ, z.
The origin of the frame is on the solar surface at the center of the local
phenomenon considered. The positive direction of the z-axis will be taken
as pointing downward. Looking down on the surface, the positive sense of
the azimuthal angle φ will then be clockwise.

II.2.1 Evershed Flow.

The longest known local phenomenon on the solar surface are the sun-
spots. In white light they appear as dark central regions called the umbra,
surrounded by a slightly lighter ring called the penumbra. The spectral
lines originating in the umbra show splittings which are ascribed to the
Zeeman effect caused by strong vertical magnetic fields. The penumbral
lines show shifts which are ascribed to the Doppler effect caused by rapid
horizontal motions in and above the penumbra. The flow pattern is approxi-
mately symmetric about the spot axis, and is outward in the deeper penum-
bral layers and inward in the overlying chromospheric layers. We will

primarily concern ourselves with the flow pattern observed in the deepest penumbral layers, because these will most closely reflect the motions of the underlying top layers of the convection zone. Our present purpose is to obtain from the data on the geometry, the heat flux and the mass motion associated with sunspots, the boundary conditions for the thermally driven mass flow in the underlying convection zone.

II.2.1.1 Dimensions .

As noted above, the general appearance of individual sunspots in white light is that of a dark umbral region surrounded by a lighter penumbral ring. The shape of the umbral and penumbral boundaries may be quite unsymmetrical as a whole and irregular in detail. Still in most cases the best approximation for the boundaries is a circle. It is found that during a given phase of the solar cycle the ratio of the umbral radius to the external radius of the penumbra is approximately the same for spots of different sizes. This ratio is slightly larger during sunspot minimum than during sunspot maximum. The average value (Allen, 1963) is:

$$R_u/R_p = .42 \tag{4}$$

where R_u denotes the radius of the umbra and R_p the external radius of the penumbra.

The size of individual sunspots covers a wide range. The smallest spots measure about 2,000 km, and the range of penumbral radii extends continuously up to a value of 50,000 km. However, the large majority of spots will have external penumbral radii in the range of 5,000 to 15,000 km.

When seen close to the limb of the solar disk, the umbra is seen to lie below the level of the average photosphere. This depression of the umbral layers is known as the Wilson effect. Accordingly the penumbral surface is not flat, but actually more of a conical nature. The inclination with the horizontal plane is generally not more than a few degrees.

28

II.2.1.2 Energy Flux .

The dark appearance of sunspots observed in white light signifies that the umbral and penumbral energy fluxes are smaller than those of the surrounding unperturbed photosphere. The distinction of umbral and penumbral regions is meaningful because of the sharp contrast at the boundaries of these regions with each other and with the surrounding photosphere. Inside each region, the effective temperature variation is much less than the temperature difference with the adjacent region. For the larger spots, the relative value of the umbral and penumbral energy fluxes is found (Allen, 1963) to be:

$$q_u/q_\odot = .27 \tag{5a}$$

$$q_p/q_\odot = .78 \tag{5b}$$

where q stands for the energy flux and the subscripts u, p and $\odot$ denote the umbra, the penumbra and the unperturbed photosphere, respectively.

When observed in white light at moderate spatial resolution, the penumbra resolves into radially-oriented bright filaments against a darker background. Typically, these penumbral filaments have a 30-minute lifespan. There is also recent evidence for transient phenomena in sunspot umbras which affect the umbral energy flux. These are explosive eruptions known as umbral flashes. The values for the energy fluxes given in Equations (5) refer to periods long compared with the time scale of these transient phenomena. Our model for the energy flux around sunspots is thus characterized by three regions with uniform energy flux, the magnitude of which decreases stepwise from its photospheric to its umbral value.

II.2.1.3 Mass Flow .

The main characteristics of the steady mass flow in sunspot penumbras are that the flow is in general predominantly horizontal, predominantly radial and in the deeper layers always directed away from the center of the spot. The observed Doppler shifts of the penumbral absorption lines show a correlation with line strength which indicates that the outward velocities

increase with depth (St. John, 1913). The strongest lines show little or no displacement, the weakest lines originating in the deepest observable penumbral layers show the largest shifts. The downward increase of the velocity is also inferred from the correlation of the observed line shifts with the position of the spot on the solar disk (Michard, 1951).

The magnitude of the observed velocity depends on the size of the sunspot. For the smaller spots the observed velocities increase approximately linearly with spot area, for the larger spots the velocities seem to reach an asymptotic value. We adopt for the magnitude of this asymptotic value:

$$v_p = 4 \text{ km/sec} \tag{6}$$

This number represents maximum velocity associated with the penumbral outflow in a large sunspot.

The longest standing controversy regarding the fine structure of the penumbral outflow concerns the horizontal boundaries of the flow. One view holds that the penumbral outflow stops abruptly at the outer edge of the penumbra (Evershed, 1909, 1910; Beckers, 1968), the other view asserts that the outflow extends well into the surrounding photosphere and there disappears gradually and smoothly (St. John, 1913; Kinman, 1952). A second controversy regards the relation between the outflow and the filamentary structure of the penumbra. Both the dark and the bright regions have been identified as the exclusive location of the penumbral outflow (Beckers, 1968; Schröter, 1965).

Quantitative measurements on the radial dependence of the outflow are available for several individual spots (Kinman, 1952; Holmes, 1960, 1963; Servajean, 1961; and Mamadazimov, 1972). In general the velocity has low values near the penumbral edges and reaches a maximum in between. The location of the maximum seems to vary from one spot to another and also depends on the angle of observation (Brekke and Maltby, 1963).

In some individual sunspots the penumbral outflow exhibited a significant azimuthal component. All attempts to find vertical velocities in the penumbra have been in vain; invariably the shifts in the penumbral lines disappear as the sunspot nears the center of the solar disk.

The general picture of the penumbral flow which we adopt is that of a strictly horizontal and predominantly radial outflow covering the entire penumbra, characterized by low velocities at the edges and a maximum near the halfway point.

II.2.2 Supergranulation.

The second and more recently discovered type of local flow is a network of polygonal cells which covers the entire solar surface (Leighton, et al., 1961). In each individual cell the solar material flows away from the center and towards the edges. The circumstance that this flow is not associated with any observable differences in brightness and that the velocities involved are much smaller than for the Evershed flow accounts for its remaining hidden for such a long time.

A further difference from the Evershed flow is that the supergranular flow is non-steady. New supergranules continually replace the older ones which have existed for a short period of time. Whereas the supergranulation as a whole is in a steady state, individual supergranules must be considered as transient phenomena.

The supergranular flow is generally ascribed to the presence of a vortex ring in the convective region below the solar surface. The central regions of the cell are thought to rise, whereas the flow near the vertical boundaries with surrounding cells is directed downward. Such a circulation will give an outflow of material on the observable surface, as is required.

In the following sections the boundary conditions regarding the geometry, the energy flux and the mass flow of the supergranular vortex ring are obtained from the available observations on individual supergranules.

II.2.2.1 Dimensions .

The supergranular network is a close packing of individual supergranular cells. This picture emerges from two-dimensional spectroscopic measurements and from observations on the chromospheric calcium network. Thus individual cells will have a polygonal horizontal cross section. The horizontal size of the cells may be characterized by an effective supergranular radius R_s. This radius is found not to vary greatly from one cell to

31

another. Values for the radius generally fall within the range 10,000 to 20,000 km, with an average value converging on 16,000 km. Thus we adopt for the effective radius for the horizontal cross section (Noyes, 1967) of a typical supergranule:

$$R_s = 16,000 \text{ km} \tag{7}$$

The range of values for supergranular radii lies well within the range of values for sunspots radii.

II.2.2.2 Energy Flux.

With the very highest spatial resolution available, the photosphere resolves into small bright patches separated by narrow dark lanes. This pattern is called the granulation. An average granule measures about 700 km so that there are many granules in each supergranule. Individual granules have a lifetime of about six minutes, which is much shorter than the lifetime of the supergranules.

On the granular level the energy flux of the solar surface is no longer uniform. The local energy flux is obtained by averaging over an area containing many granules or over a period spanning many granular lifetimes. This average local energy flux does not vary from one supergranule to another or within the surface of a given supergranule. Because of the close packing of the cells, the magnitude of the supergranular energy flux $q_\odot$ equals the entire solar luminosity divided by the entire surface area. This gives (Allen, 1963):

$$q_\odot = 6.41 \times 10^{10} \text{ erg/cm}^2\text{sec} \tag{8}$$

II.2.2.3 Mass Flow.

The supergranular flow shows a general resemblance to the penumbral outflow but is much slower than the latter. The flow is horizontal as witnessed by its being undetectable at the center of the solar disk. For cells away from the center lines originating in the near side are invariably blue shifted, lines from the far side of the cell invariably show a red shift.

This bears out that the flow is oriented from the center of the cell towards the edges. Azimuthal velocities of any consequence do not seem to be present. For the maximum value of the outward velocity (Noyes, 1967) we adopt:

$$v_S = .4 \text{ km/sec} \tag{9}$$

This is a full order of magnitude less than the maximum outward penumbral flow in a sunspot of comparable size.

The position of the velocity maximum seems to be close to the boundary of the cell. In the central region of the cells the outflow velocities appear to be small.

The model which we adopt for the supergranular flow is a strictly horizontal, predominantly radial outflow which peaks close to the boundary and has low velocities in the central region of the observable surface of the cell.

III STRUCTURE OF THE SOLAR INTERIOR

The internal constitution of the sun and of stars in general cannot be determined by direct observation, but instead has to be derived from physical principles. This approach has led to a detailed understanding of the structure and evolution of stars beginning with their free fall contraction from the interstellar gas to their final stages as a white dwarf or a neutron star. One simplification that generally has to be made is the exclusion of rotation and of magnetic fields. Over the years opinion as to the effect of this simplification has fluctuated; the current opinion is that rotation and magnetic fields will not drastically alter stellar structure and evolution as presently understood (Clayton, 1968). Accordingly, we will retrace the rotational history of the sun in the framework of the usual evolutionary stages of a star of one solar mass.

From its initial condensation to the present the solar material has continuously been in a gaseous state. The four parameters specifying this state are the composition, the mass density, the temperature and the pressure. The composition refers to the distribution of the constituents of the gas over the different nuclear species. This distribution is assumed to be spatially homogeneous in the initial cloud, but in the course of the subsequent nuclear burning stages the composition develops spatial inhomogeneities which stabilize rotation patterns with negative radial angular velocity gradients (Goldreich and Schubert, 1968). In the course of the contraction the emerging balance of gravitational and pressure forces imposes an inwardly-increasing pressure throughout the star. Soon the central pressure is many orders of magnitude above the surface pressure, and similar, though smaller differences in central and surface temperature and density develop as a consequence of the virial theorem.

The development of an inhomogeneous temperature distribution will necessarily lead to heat transfer. Up to the present evolutionary stage of the sun, the two domianant processes are radiative and convective energy

transfer. The former takes place when the local temperature gradient in a layer is below the corresponding adiabatic value. If the temperature gradient is superadiabatic then the layer is convectively unstable. This is the Schwarzschild criterion for convective instability. The energy is then carried by vertical motions of convective elements.

With regard to the rotational evolution of the sun, the question now is what the rotational state of the initial gas cloud was, and how this state was affected by the subsequent evolutionary stages comprising contraction with central concentration, and energy release with radiative and convective energy transfer. For the rotational state of the initial gas cloud a simple and reasonable approximation is to assume a uniform mass distribution and a uniform intrinsic rotation rate roughly equal to the orbital rotation rate about the galactic center (Mestel, 1969). During the early optically thin phases of the contraction the gas is so tenuous that viscous forces are negligible, so that angular momentum is conserved locally. In other words, the vortex lines are completely frozen into the material. The central regions where mass accumulates would thus also acquire the highest rotation rates, which would eventually lead to a rapidly rotating core for the present sun.

During the intervening radiative and convective phases of the sun orbital angular momentum about the rotation axis is not conserved locally. In the radiative case, hydrostatic and radiative equilibria require the formation of meridional circulations in the stellar interior which will redistribute the angular momentum. In the convective case the momentum exchange is so much enhanced by turbulence that the viscous forces can no longer be neglected. If the surface of the star is convective there is the further possibility that the angular momentum is not even conserved globally because of mass loss and stellar wind torques. The quantitative effect of the above processes on the rotation pattern is quite uncertain, particularly in view of the poorly understood behavior of the magnetic field during the period of star formation. As in the earlier discussions, this aspect of stellar structure will be left out in the following considerations on the rotational history of the sun.

III.1 Physical Conditions .

On the microscopic level the constituents of the stellar gases inter-
act with each other through electromagnetic forces. Under normal stellar
conditions this interaction rapidly leads to the establishment of an equi-
librium distribution of the random motions of the molecules and photons
which are present. By molecules we mean any kind of ion, electron or neu-
tral atom or molecule. The random motions of the constituents bring about
an external pressure on the surroundings of each volume element of stellar
gas; both the material particles and the photons contribute to this pres-
sure. For conditions which have occurred during the solar evolution, radia-
tion pressure can be neglected compared with the particle pressure, and of
the latter, the kinetic pressure dominates the pressure due to Coulomb-
interaction of the charged constituents of the gas. During the same epoch,
kinetic energy transfer in the form of heat conduction has been negligible
compared with radiative and convective energy transfer.

III.1.1 Local Thermodynamic Equilibrium.

An indispensable simplification in the description of the state of
stellar material is the assumption that the energy distribution of all con-
stituents is characterized by a local temperature and that the spatial dis-
tribution of the temperature is the same for all constituents. Under nor-
mal circumstances the interactions among constituent particles and photons
will be strong enough to establish local thermodynamic equilibrium on a
time scale much shorter than that of the secular evolutionary changes. An
exception to this rule occurs on the surface of the star, where the photons
decouple from the stellar material and take off through the transparent at-
mosphere.

The state variables of a gas in local thermodynamic equilibrium are
related by simple equations. The simplest case is that the kinetic
pressure depends only on the mass density of the gas. This relation is
called the polytropic or barotropic relation. The more general case is
that the pressure depends on both density and temperature, and, if chemical
or nuclear reactions occur, also on the composition of the gas through the
mean molecular mass. Writing P, ρ, T and μ for the pressure, density,

temperature and mean molecular mass respectively, the two relations can be written as:

$$\text{polytrope}: \quad P = K\rho^{(n+1)/n} \tag{1a}$$

$$\text{ideal gas}: \quad P = \frac{k}{m_H}\frac{\rho T}{\mu} \tag{1b}$$

where in (1a) n denotes the polytropic index and in (1b) k and m_H are Boltzmann's constant and the atomic mass unit respectively.

As regards the energetic constitution of the stellar gas there is an essential difference between the fully ionized and the partially ionized states. In the first case the only form of internal energy of the gas resides in the random motions of the constituent particles. In an equilibrium state the internal energy density is then uniquely determined by the pressure. The situation is different if neutral atoms are present which provide an extra degree of freedom to the internal energy in the form of the ionization potential. According to Saha's equation, the degree of ionization depends both on the pressure and on the temperature. Because of the contribution from the ionization potential, the internal energy then also depends on both the pressure and the temperature. Writing U for the internal energy per unit volume we have for the respective cases:

$$\text{fully ionized:} \quad U = \frac{3}{2} P \tag{2a}$$

$$\text{partially ionized:} \quad U = U(P,T) \tag{2b}$$

We have been unable to find an explicit form for Equation (2b) expressing the dependence of the internal energy density on pressure and temperature or composition valid for the solar gas. The lack of such an equation will be found to preclude a quantitative theoretical estimate of the thermomechanical effect which will be discussed in Chapter IV.

III.1.2 Hydrostatic Equilibrium .

Soon after the initial free fall of the original gas cloud the pressure forces building up inside it begin to restrain and eventually balance the

gravitational pull. This happens long before the final main sequence radius of the star has been reached. The larger part of the contraction towards the main sequence is characterized by the balance of kinetic pressure and inward gravity, a balance which may be expected to hold even better during the main sequence lifetime of the star.

The above picture underlies the calculation of stellar structure during this evolutionary period, and we assume that the inclusion of rotation does not drastically alter this picture. Before formulating the condition of hydrostatic equilibrium explicitly, we first note that this term strictly applies only to situations without any mass motions. In the present case the concept is broadened to include purely rotational motions only; in other words, the fluid velocities are allowed to have azimuthal components, but not radial or polar components. In this case the only extra force which has to be incorporated in the force balance is the centrifugal force due to the rotational motion. If motions in meridional planes occurred in combination with rotation there would be additional inertial forces in the form of the Coriolis force.

For the case of a rotating gas cloud the condition of hydrostatic equilibrium thus has a kinematical and a dynamical part, the first one ruling out any mass motion in meridional planes and the second one balancing the gravitational-, pressure- and centrifucal forces. The kinematic condition can be stated in the form that the curl of the fluid vorticity vanishes. In other words, in a gas cloud in hydrostatic equilibrium in the sense defined above there can be no closed vortex lines. Any axisymmetric meridional motion would necessarily result in closed stream lines, which would constitute an azimuthal vortex ring, contrary to the imposed kinematic condition. In terms of the mass density ρ, the pressure P, the gravitational potential $\emptyset$, the fluid velocity $\vec{v}$ and the vorticity $\vec{w} \equiv \vec{\nabla} \times \vec{v}$ the two conditions for hydrostatic equilibrium take the form:

$$\vec{\nabla} \times \vec{w} = 0 \tag{3a}$$

$$\vec{v} \times \vec{w} - \frac{1}{2} \vec{\nabla}v^2 = \frac{1}{\rho} \vec{\nabla}P + \vec{\nabla}\emptyset \tag{3b}$$

38

With Equation (3b) the consistency of the equations of state (1a,b) and various rotation patterns with hydrostatic equilibrium can be investigated. In particular it follows that for polytropes Equation (3b) implies that the angular velocity depends only on distance from the rotation axis, i.e. equal rotation rates on cylinders. If the rotation rate is not constant on cylinders then either hydrostatic equilibrium is not fulfilled, or the fluid is not barotropic. In the first case meridional circulations will develop in violation of the kinematic condition (1a), whereas in the second case the ideal gas law (1b) has to be introduced for the equation of state. This will lead to a static baroclinic situation in which the density and temperature surfaces are inclined in opposite manner with the surfaces of constant pressure.

III.1.3 Radiative Equilibrium.

As soon as temperature differences develop inside the contracting gas cloud radiative energy transfer will set in. At first the resulting photons escape freely, but long before the pre-mainsequence contraction ceases the stellar material has become opaque and the photons can only diffuse outward driven by the outward temperature gradient. The state of radiative equilibrium is achieved when the local outward energy flux is entirely radiative. This state is unattainable for a polytrope with an arbitrary rotation pattern. As was noted in the preceding section, hydrostatic equilibrium in a polytrope demands rotation on cylinders. Different rotation patterns will be accompanied by meridional motions which in the present case will locally alter the energy transfer, in violation of the definition for radiative equilibrium.

In radiative regions the local heat flux is taken proportional to the local temperature gradient in the following form:

$$\vec{q} = -\frac{4acT^3}{3K\rho} \vec{\nabla}T \tag{4}$$

where a is Stefan's constant, c the speed of light and K the opacity. The other symbols are as defined earlier. The opacity expresses the strength of the coupling between radiation and matter in the stellar material. In

the early cool stages of the star the opacity is so large that superadiabatic temperature gradients would be required to drive all the internally released energy to the surface. At this point convective instability sets in and the energy transfer is taken over by convective motions inside the star.

III.1.4 Convective Equilibrium .

According to the Schwarzschild criterion, a fluid layer with a super-adiabatic temperature gradient is convectively unstable. This means that a fluid element undergoing an adiabatic displacement along the temperature gradient will find itself hotter than the surrounding layers and consequently more buoyant. In a horizontal layer with a vertical temperature gradient hot, rising elements will experience an upward buoyancy force which will displace them further, and cold, sinking elements will experience a downward buoyancy force with the same effect. Because of the pressure dependence of the internal energy Equation (2a,b) the vertical motions are accompanied by energy transfer. In the state of convective equilibrium the energy transfer is entirely convective.

The mixing-length theory is an attempt to describe the state of a layer in convective equilibrium in terms of concepts from kinetic theory. In analogy with the mean free path for ordinary molecules each convective parcel is treated as a "molecule" which can travel over a given distance called the mixing length before it dissolves. The mixing length is taken close to the local pressure scale height and this length also characterizes the horizontal cross section of each parcel.

For the sustenance of the convective heat flux the temperature gradient has to remain superadiabatic throughout the convective region. For practical astrophysical situations the excess temperature gradient necessary to drive the entire stellar luminosity is found to be very small, i.e. the temperature distribution is very nearly adiabatic. This means that to a good approximation the equation of state is a special case of the polytrope law Equation (1a), where now the exponent equals the first adiabatic index of the stellar gas.

The above picture is again the customary basis for calculations of stellar evolution. We assume again that the main results of these calculations are not impaired by the inclusion of rotation. Conversely, we then have to investigate the effect of convection on the rotation pattern. In this matter a specific proposal has been made (Biermann, 1951). It is argued that because of the preferred direction of gravity the turbulent momentum exchange is anisotropic. Depending on the degree of anisotropy, the orbital angular velocity would increase more or less rapidly inward, the limits being a uniform rotation for isotropic turbulence (s = 1) and an inverse square dependence on radius for purely monotropic turbulence (s = 0), viz:

$$\Omega = \frac{\Omega_0}{(r/R)^{2(1-s)}} \tag{5}$$

where Ω_0 and R denote the angular velocity and the radius of the surface respectively. Rotation patterns of the form (5) do not satisfy the hydrostatic equilibrium condition (3b) if the fluid is barotropic. Consequently meridional motions develop which alter the pattern (5). The rotation patterns which are found from more elaborate hydrodynamical treatments possess latitude-dependent rotation patterns if the turbulent momentum exchange is non-isotropic (Kippenhahn, 1963; Sakurai, 1966; Köhler, 1970).

III.2 Past .

In the previous section we have discussed the physical principles which are involved in the evolution of the sun up to its present state. This approach led to the view that this evolution divides into two phases, namely the quasistatic contraction of the initial gas cloud, and the main sequence phase. The two phases are distinguished by their sources of energy: during the contraction the source of energy is mostly gravitational and during the main sequence nuclear reactions sustain the energy output. The main sequence phase lasts much longer than the contraction phase. It appears however that the relatively short lived contraction phase has the more important effect on the rotational evolution of the star.

An indication in this direction comes from observational astronomy. It is found that the observed surface rotations of stars are correlated with the spectral type in such a way that young stars generally have high rotation rates, while more mature stars have lower rotation rates by as much as a factor of fifty. The sun, being a middle-aged star with a well-developed convection zone, has with 2 km/sec, one of the lowest observed surface velocities. The transition from rapid rotators to slow rotators occurs in stars of a spectral type possessing extended convective envelopes. The theoretical predictions of the evolution of an individual star can thus be tested against the statistical picture emerging from observations made on a large number of different stars.

II.2.1 Hayashi Phase.

It is now known that during the larger part of its contraction towards the main sequence, the sun was fully convective. In the course of this contraction and the concomitant rise in central temperature a gradual transition from gravitational to nuclear energy release took place, until the latter became large enough to sustain the full luminosity and halt the contraction. At this point the sun has reached the main sequence.

The observations on stellar rotations do not bear out whether the deceleration of the surface takes place largely during the Hayashi phase or whether a significant slowing down occurs also during the main sequence lifetime of the star. Two different mechanisms have been proposed by which the surface might be slowed down from within during the Hayashi phase. In one approach, the effect of Coriolis forces on vertical convective motions is considered, where the convective elements are treated as point masses. If the motions are purely vertical then the angular velocity is found to follow an inverse square dependence on distance from the center, as in Equation (5) for the case $s = 0$ (Biermann, 1951). The resulting redistribution of angular momentum would be characterized by a significant slow down of the surface and a small increase in rotation rate of the core because of the central concentration of mass. A more radical proposal is that vorticity would be expelled all together by convection (Gough and Lynden Bell, 1968). In this view the sun would have lost the bulk of its angular velocity

during the Hayashi phase, and would presently possess a slowly rotating interior.

The alternative possibility is that the solar surface has been slowed down by an external torque. Considerable mass loss or very large stellar wind torques would be required to reach the observed terminal rotation rates during the Hayashi phase. In this view it would be more likely that the sun arrived on the main sequence with much of its initial rotation, which was then gradually reduced by the solar wind torque to the present low value (Dicke, 1970).

III.2.2 Main Sequence.

Soon after the transition from gravitational to nuclear energy release has been completed a radiative core develops in the stellar interior. This happens because the increased central temperatures have decreased the opacity of the stellar material to a point where an outward radiative flux balancing the energy release can be driven outward by means of a sub-adiabatic temperature gradient. With increasing age the radiative core grows gradually at the expense of the surrounding convective layers.

The newly formed radiative layers inherit a rotation pattern which is not likely to alter drastically from within during the following main sequence period. On the one hand both diffusive angular momentum transfer due to shear, and convective momentum transfer due to meridional circulation, do not seem to alter the rotation pattern significantly during the main sequence lifetime (Cowling, 1953; Mestel, 1965). On the other hand the nuclear reactions lead to gradients in the mean molecular mass which will stabilize rotation patterns characterized by large negative angular velocity gradients (Goldreich and Schubert, 1967). Furthermore, the surface torques exerted by the solar wind seem to be too small to change the total angular momentum of the sun appreciably during the main sequence lifetime (Dicke, 1970).

The solar wind torque may still account for the slow surface rotation of the sun if only a part of the solar interior would have been affected by it. This picture receives some quantitative support from observations on the rotation rate of young main sequence stars.

III.3 <u>Present</u> .

In its present evolutionary stage the solar interior consists of a radiative core surrounded by a convective envelope whose thickness has by now shrunk to a fraction of the total solar radius. For this thickness we will adopt a value of 200,000 km, or approximately .29 of the total radius. This value is used in the most eleborate model of the solar convection zone available to us (Baker and Temesvary, 1966). For the present constitution of the radiative core of the sun we adopt the model given by Strömgren (re-produced in Clayton, 1968). These models do not include the effects of rotation in any stage of the evolution. Any such effects in the real sun are again assumed not to have altered the overall evolutionary picture and the present state to any great extent.

A few words must be said about the solar atmosphere. The surface of the sun coincides with the upper boundary of the convection zone. The convective motions are thought to have important effects on the structure of the solar atmosphere. In particular they are held responsible for the formation of the solar corona and indirectly for the solar chromosphere. Together with the photosphere, these layers provide important observational clues towards the understanding of the rotation below the surface, so that in the end of the present chapter we will include a short discussion on their structure and their relation to the underlying convective layers.

III.3.1 <u>Radiative Core</u> .

The radiative core of the present sun extends to .71 of the solar radius in the adopted model. It comprises 99% of the total solar mass, and the entire solar luminosity is generated inside it. More precisely, more than 99% of the solar luminosity is generated within .3 of the solar radius. The source of energy is the fusion of protons into helium nuclei. The central temperature is 1.6×10^{7} °K, which has fallen off an order of magnitude at the surface of the radiative zone. With a value of 160 gr/cm^{3} the central density is three orders of magnitudes higher than the surface value. According to the ideal gas law the pressure stratification in the radiative region will then amount to four orders of magnitude. At the center the weight fraction of hydrogen in the solar gas has decreased from an assumed
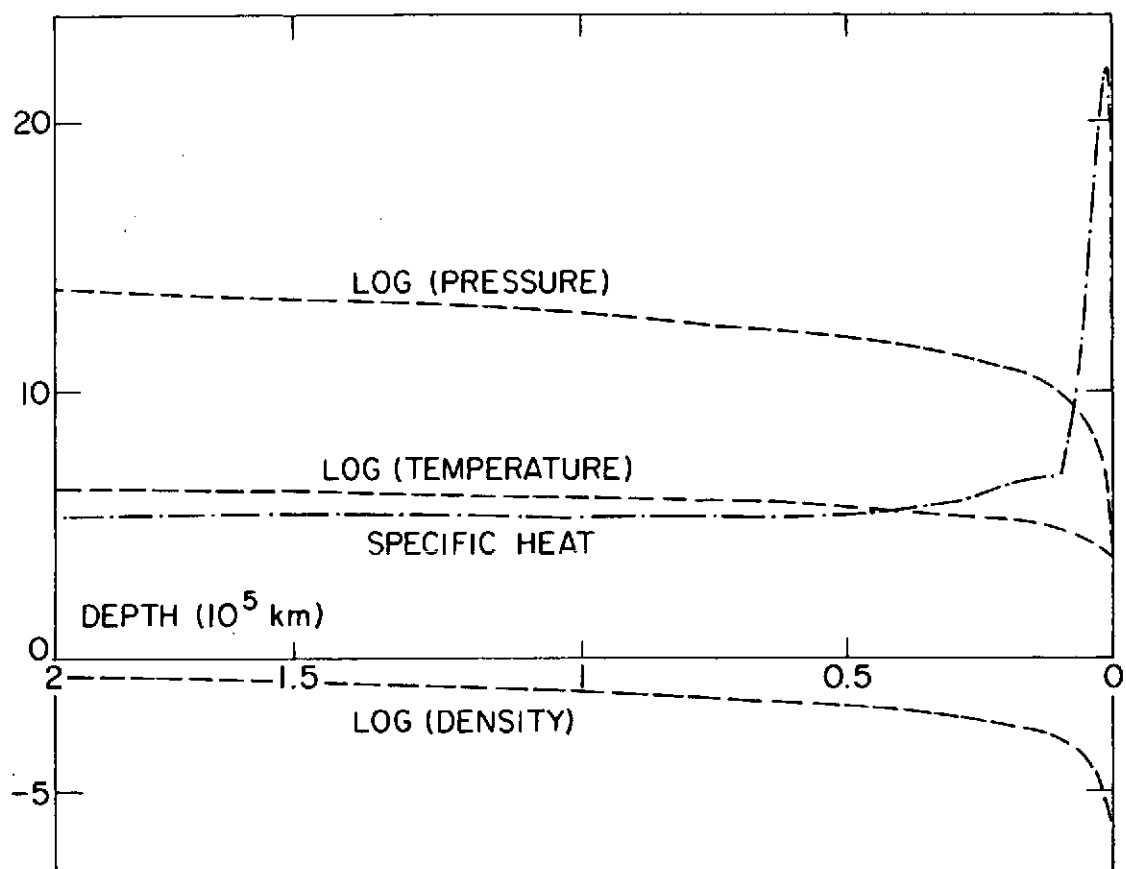
Figure 3. Dependence of pressure, temperature, density
and specific heat at constant pressure on
depth in the solar convection zone.

initial value of .71 to a value of .36. This amount of compositional stra-
tification is large enough to stabilize central rotation rates up to twenty
times faster than the surface rotation.

III.3.2 Convective Envelope .

Although in the adopted model the convective regions comprise only .29
of the solar radius, the convective layers are more stratified than the more
extensive radiative region. In other words, the scale heights of the state
parameters have decreased outward. The top and bottom pressures, densities
and pressures are now respectively approximately nine, six and two orders
of magnitude apart. In the adopted model the assumed weight fraction of
hydrogen is .70, 1% below the value assumed in the adopted model for the
radiative core.

The general dependence of the state parameters is represented in Fig-
ure 3, which also includes the relative specific heat at constant pressure.
This last quantity shows the effect of the gradual deionization which occurs
in the top layers of the convection zone. The first noticeable raise in
the specific heat occurs at about 30,000 km below the surface and is due to
the deionization of fully ionized helium. The sharp peak in the specific
heat due to partially ionized hydrogen lies at 1,800 km below the surface.

From bottom to top of the convection zone the pressure schale height
decreases from about 80,000 km to about 300 km. With these values the number
of convective parcels which are present on the respective boundaries of the
convective envelope can be estimated using the earlier described mixing-
length picture of convective equilibrium. On this basis there are an aver-
age of 140 convective parcels present on the inner boundary, and several
million on the outer visible surface of the envelope. On the 30,000 km level
an average of 9,000 parcels are present.

III.3.3 Atmosphere .

The structure of the solar atmosphere is determined by factors quite
different from the ones discussed so far. The following discussion is based
not so much on physical principles as on direct observation of the features
involved.

In the first place the temperature is found to increase with height above the solar surface over a distance of several thousand kilometers. The hottest layer is the corona, with temperatures of several million degrees, below it directly above the photosphere are the chromospheric layers characterized by temperatures around 10,000°K. All three layers have their own distinctive spectral lines, the photosphere being characterized by a large number of absorption lines from numerous elements, the chromosphere by emission lines in hydrogen and calcium and the corona by emission lines from highly ionized metals. These identifications were used in obtaining a model of the atmospheric rotation pattern in Chapter II.

A second aspect of the solar atmosphere is the important effects which are connected with, or due to, the observed magnetic fields. As far as the effects on the atmospheric rotation are concerned, we adopt the following picture. At the top of the convection zone the large scale magnetic field is concentrated by the supergranular motion at the corners where individual supergranules meet. Above the surface the vertical magnetic flux tubes spread out into the solar atmosphere to form an effectively uniform field in the corona which couples the coronal gas mechanically to the top of the convection zone. At the lower chromospheric levels this coupling is less developed because of the smaller spreading of the magnetic flux tubes and also because substantial numbers of neutral atoms are present. Because of the narrow boundaries between supergranules compared to their size the photospheric layers are assumed to be unaffected by the vertical flux tubes which emerge from the convection zone. The above picture is adapted from the discussion of the supergranulation given by Noyes (1967).

Beyond the corona there is an outward mass flow extending into interplanetary and interstellar space known as the solar wind. At the present time the solar wind seems to brake the convective layers with an e-folding time longer than the main sequence lifetime of the sun (Dicke, 1970). In that case the solar wind torque must have been larger in the past, if it is to explain the present slow surface rotation. This could be associated with the increased magnetic activity usually associated with younger stars.

IV DYNAMICAL EQUATIONS FOR THE SOLAR CONVECTION ZONE

In the preceding chapter we presented the standard mixing length description of the solar convection zone. This description specifies the thermodynamic state of the convection zone in the absence of rotation. The additional description of the rotational state of the solar convection zone in the framework of the mixing length theory can be made through a formalism which is developed in the present chapter.

The discussion of mixing length fluids proceeds on three levels which are characterized by three different length scales. On the microscopic or molecular level the properties of individual atoms and molecules are considered. In fully ionized regions the basic constituents of the solar plasma behave as point masses which can exchange kinetic energy through the Coulomb-interaction. If partial ionization is present the molecules have, due to the ionization potential, also an internal energy which can be exchanged in collisions.

On the intermediate level the properties of individual convective parcels are considered. On this level the length-scale is one mixing length. Each parcel will contain a very large number of atoms and molecules. An indispensable tool for the description of such ensembles of molecules is the assumption of local thermodynamic equilibrium. This implies that the state of the material inside every parcel can be specified with the usual thermodynamic variables for a hot gas, i.e. pressure, temperature, density and composition. Furthermore there will be a kinetic equation of state for the pressure and a caloric equation of state for the internal energy. For complete ionization the random kinetic energy of the atoms determines both the internal energy density and the pressure, but with partial ionization there is a contribution to the internal energy from the ionization which depends on other variables besides the pressure (Saha's equation).

On the large scale level one considers the behavior of large numbers of convective parcels. The typical length-scale is here the linear

dimension of the convective region. On this level one seeks to relate the
properties of individual parcels to those of the "mixing length fluid."

IV.1 Dynamics of Mixing Length Parcels.

In the standard mixing length picture of convective heat transfer con-
vective parcels travel over a vertical distance called the mixing length   L
between their formation and their dissolution. The mixing length   L   is
taken to be close to the local pressure scale height H_p:

$$L = \alpha H_p \qquad\qquad\qquad IV.1$$

In the solar model of Chapter III the parameter α had the value 1.5.

The translatory motion of a convective parcel is determined by the
balance of the buoyancy force on it and its inertia. The average vertical
velocity of a parcel can be found from this balance to be

$$v^2 \approx gL \frac{\Delta T}{T} \qquad\qquad\qquad IV.2$$

where   g   is the local gravitational acceleration and ΔT is the average
temperature difference between the parcel and the ambient fluid.

We propose that in addition to the vertical buoyancy force on a parcel
there will be a buoyancy couple on it which will rotate the parcel about a
horizontal axis through its center of mass. This couple arises from the
redistribution of mass inside a parcel which has undergone an adiabatic
infinitesimal rotation about a horizontal axis. After such a rotation, the
center of mass of the parcel no longer coincides with its geometrical cen-
ter as defined by its spherical surface. If the temperature gradient in
the parcel is superadiabatic, the displacement of the center of mass with
respect to the geometrical center is such that the resulting buoyancy couple
will rotate the parcel further. Thus in superadiabatic fluid layers not
only translational but also rotational instability exists. Every convective
parcel will acquire during its lifetime linear momentum from the buoyancy
force on it and intrinsic angular momentum from the buoyancy couple on it.
A crude estimate of the average rotation rate ω of a parcel can be obtained

obtained by substituting $\omega = v/L$ in IV.2, giving:

$$\omega^2 \approx \frac{g}{L} \frac{\Delta T}{T} \quad . \tag{IV.3}$$

Thus to an even larger extent than with the convective velocities the convective rotation rates are highest at the top of the convection zone, where the mixing length L and the temperature are T lowest and the temperature difference ΔT between parcels and ambient fluid is highest. For a more detailed derivation of this relation, see Appendix A.

We describe the proposed internal rotations by means of a spin vector $\vec{\omega}$ which represents the intrinsic rotation rate of each individual parcel. If the rotational motions of adjacent parcels do not interact with each other, the spins will be randomly oriented in horizontal planes. On the other hand, if there is a sufficiently strong interaction between spins they may organize themselves into local symmetric patterns. A third possibility is that the spins of all convective parcels are aligned with some external force on them.

The latter case will occur when the convective fluid layer under consideration has an external rotation. In that case all parcels start out with an intrinsic rotation rate given by one-half of the vorticity of the ambient fluid. The expansion and contraction during a parcel's lifetime will change the parcel's moment of inertia and the parcel will have to spin up or spin down in order to conserve its original angular momentum. If the volume change of a parcel is spherically symmetric then the rotation axis will remain parallel to the direction of the original vorticity, or:

$$\frac{1}{2} \vec{\nabla} \times \vec{v} = \xi \vec{\omega} \tag{IV.4}$$

With the aid of the "expanding sphere" model of convective parcels the range of the parameter ξ can be estimated from standard mixing length theory to be:

$$e^{-\frac{2\alpha}{3\Gamma}} \lesssim \xi \lesssim e^{\frac{2\alpha}{3\Gamma}} \tag{IV.5}$$

where α is the ratio of the mixing length L to the local pressure scale height, equation IV.1, and Γ is the first adiabatic index of the material

50

which forms the parcel. If this material is an ideal gas, the adiabatic index has the value $\Gamma = 5/3$ and with $\alpha = 1.5$ the parameter ξ lies between the values .55 and 1.8. In a partially ionized region Γ may go down to 1.1, and the range of ξ is then between .42 and 2.4. In either case a mixture of rising and sinking parcels should have an average ξ close to unity, with $\xi > 1$ representing a predominance of hot rising parcels and $\xi < 1$ representing a predominance of cold sinking parcels. The validity of equation IV.5 is restricted to situations in which buoyancy couples on individual parcels can be neglected compared with the coriolis couples which they experience in corotating coordinate frames. A more detailed derivation of equation IV.5 can be found in Appendix B.

IV.2 Dynamics of Mixing Length Fluids.

In a superadiabatic layer comprising many pressure scale heights a large number of convective parcels will be present at any given time. The behavior as a fluid of such a layer will be determined by the properties of the convective parcels which form its "molecules." As a model for these molecules we have adopted the "expanding sphere" model described in the previous section. We have assumed that these expanding spheres possess spins which can interact with each other or with external forces.

The molecular models used to describe ordinary fluids generally allow only central forces between interacting molecules. Kinetic theory then brings out that in fluids consisting of central force molecules, the forces on the surface of a volume element of fluid can be completely described with a stress vector. In other words, a small surface element in an ordinary fluid will experience a force which will tend to displace it, but no couples which will tend to rotate it. In fluid dynamics this principle is known as Cauchy's stress principle. In terms of a stress tensor $\overset{\leftrightarrow}{\tau}$ and a couple stress tensor $\overset{\leftrightarrow}{\mu}$ it can be stated in the form that the couple stress tensor vanishes and the stress tensor is symmetric:

$$\overset{\times}{\tau} = 0 \ , \ \overset{\leftrightarrow}{\mu} = 0 \qquad\qquad \text{IV.6a}$$

or

$$\tau_{ij} = \tau_{ji} \ , \ \mu_{ij} = 0 \qquad i,j = 1,2,3 \qquad \text{IV.6b}$$

Cauchy's principle leads to an adequate description of most ordinary fluids.

We propose that Cauchy's (Mase, 1970) principle is not valid in mixing length fluids, the reason being that the spins which we ascribe to each

convective molecule will generally interact with forces which need not be central. Rather, the spins should interact with short range, non-central forces which introduce couple stresses on an arbitrary surface element in the fluid as well as an anti-symmetric component in the stress tensor. In addition we make the hypothesis that the couple stress tensor $\overleftrightarrow{\mu}$ should be symmetric. The above conditions can be expressed in terms of the stress tensor $\overleftrightarrow{\tau}$ and the couple stress tensor $\overleftrightarrow{\mu}$ as:

$$\overleftrightarrow{\tau} \neq 0 \ , \ \overleftrightarrow{\mu} = 0 \qquad \qquad \text{IV.7}$$

or

$$\tau_{ij} \neq \tau_{ji} \ , \ \mu_{ij} = \mu_{ji} \qquad i,j = 1,2,3 \qquad \text{IV.8}$$

As with the Cauchy principle IV.6 the validity of equation IV.8 is to be inferred from the manner in which convective molecules interact or from the macroscopic results which derive from them. The remainder of this chapter concentrates on the second course.

We now proceed to formulate the dynamical equations for a superadiabatic layer as those of a fluid possessing three translational and three rotational degrees of freedom which are subject to stresses and couple stresses. The effect of the stresses depends on the mass distribution of the fluid, the effect of the couple stresses depends on the distribution of moment of inertia in the fluid. External forces (such as gravity) are assumed known and are omitted from the following formulation of the balance equations. We present the balance equations in local form because they yield most easily the steady state forms in which we are eventually interested.

The continuity and momentum equation in our formulation for mixing length fluids retain their familiar forms:

$$\frac{\partial \rho}{\partial t} + \vec{\nabla} \cdot \rho \vec{v} = 0 \qquad \qquad \text{IV.9}$$

$$\frac{\partial \rho \vec{v}}{\partial t} + \vec{\nabla} \cdot (\rho \vec{v} \vec{v} + \overleftrightarrow{\tau}) = 0 \qquad \qquad \text{IV.10}$$

52

Each equation says that there are no sources or sinks for mass or momentum and that an increase in mass or momentum density at a given point is wholly due to an influx of these quantities from outside. In the case of the momentum this in- or outflux can be either convective and reversible (as for the term $\rho \overleftrightarrow{vv}$ or diffusive and irreversible (contained in the stress tensor $\overleftrightarrow{\tau}$).

In addition to mass and momentum also the moment of inertia and the total angular momentum are to be conserved in the absence of external forces. Writing Θ for the specific moment of inertia and $\vec{L}, \vec{S}, \vec{J}$ for specific orbital, intrinsic and total angular momentum respectively, we have:

$$\frac{\partial \rho \Theta}{\partial t} + \nabla \cdot \rho \vec{v} \Theta = 0 \qquad\qquad \text{IV.11}$$

$$\vec{J} = \vec{L} + \vec{S} = \vec{r} \times \vec{v} + \Theta \vec{\omega} \qquad\qquad \text{IV.12}$$

$$\frac{\partial \rho \vec{J}}{\partial t} + \vec{\nabla} \cdot (\rho \overleftrightarrow{vJ} - \overleftrightarrow{\tau} \times \overleftrightarrow{r} + \overleftrightarrow{\mu}) = 0 \qquad\qquad \text{IV.13}$$

Again the change in moment of inertia density and total angular momentum density in the fluid is entirely due to in- or outflux of these quantities. The dyadic $\rho \overleftrightarrow{vJ}$ represents the convective, reversible part of the total angular momentum flux, the tensors $\overleftrightarrow{\tau} \times \vec{r}$ and $\overleftrightarrow{\mu}$ contain the diffusive, irreversible part of the angular momentum flux. The term $\overleftrightarrow{\tau} \times \vec{r}$ brings about changes in the orbital part of the angular momentum, the term $\overleftrightarrow{\mu}$ acts directly on the intrinsic part of the angular momentum.

Due to the presence of an anti-symmetric part in the stress tensor the orbital and intrinsic part of the angular momentum are not conserved separately. This can be seen by investigating the orbital momentum balance separately by multiplying the moment balance IV.10 vectorially with the position vector $\vec{r}$. After rearranging and subtracting from the total angular momentum balance IV.13 one finds:

$$\frac{\partial \rho \vec{L}}{\partial t} + \nabla \cdot (\rho \overleftrightarrow{vL} - \overleftrightarrow{\tau} \times \vec{r}) = \vec{\tau} \qquad\qquad \text{IV.14}$$

$$\frac{\partial \rho \vec{S}}{\partial t} + \vec{\nabla} \cdot (\rho \vec{v}\vec{S} + \overset{\leftrightarrow}{\mu}) = -\vec{\tau} \qquad\qquad\text{IV.15}$$

where the pseudovector $\vec{\tau}$ represents the anti-symmetric part of the stress tensor. The components of this vector act as sources and sinks of orbital and intrinsic angular momentum. In a given volume element these quantities can increase or decrease not only through convective or diffusive in- or outflux through the walls, but also through creation or destruction inside the volume element itself. This conversion of orbital into intrinsic angular momentum or vice versa under conservation of the total angular momentum can be properly termed an example of spin-orbit coupling.

The fifth and last balance equation refers to the conservation of energy. In a mixing length fluid we recognize three forms of energy, namely kinetic, rotational and internal energy. The internal energy will normally represent the random thermal energy present in a volume element, but may include a significant contribution from the ionization potential if partial ionization is present. Writing $\frac{1}{2}\rho v^2$, $\frac{1}{2}\rho \; \Theta \; \omega^2$ and u for the respective energy densities in the fluid we have:

$$e = \frac{1}{2}\rho v^2 + u + \frac{1}{2}\rho \; \Theta \; \omega^2 \qquad\qquad\text{IV.16}$$

$$\frac{\partial \rho e}{\partial t} + \vec{\nabla} \cdot (\rho e \vec{v} + \overset{\leftrightarrow}{\tau} \cdot \vec{v} + \overset{\leftrightarrow}{\mu} \cdot \vec{\omega} + \vec{q}) = 0 \qquad\qquad\text{IV.17}$$

As before the term $\rho e \vec{v}$ represents the flux through the wall of a volume element; the terms $\overset{\leftrightarrow}{\tau} \cdot \vec{v}$ and $\overset{\leftrightarrow}{\mu} \cdot \vec{\omega}$ represent the work done on the volume element by the stresses and by the couple stresses respectively and $\vec{q}$ represents the heat flux through the walls.

The balances of the kinetic and rotational energy can be investigated separately by multiplying the momentum balance IV.10 scalarly with the velocity vector $\vec{v}$ and the intrinsic angular momentum balance IV.15 scalarly with the spinvector $\vec{\omega}$. After rearranging using the continuity equations IV.9, 11 and the energy balance IV.17 one has for all three kinds of energy:

$$\frac{\partial \tfrac{1}{2}\rho v^2}{\partial t} + \vec{\nabla}\cdot(\tfrac{1}{2}\rho v^2\vec{v} + \overleftrightarrow{\tau}\cdot\vec{v}) = \overleftrightarrow{\tau}:\overleftrightarrow{\nabla v} \qquad\qquad \text{IV.18}$$

$$\frac{\partial \tfrac{1}{2}\rho\Theta\omega^2}{\partial t} + \vec{\nabla}\cdot(\tfrac{1}{2}\rho\Theta\omega^2\vec{v} + \overleftrightarrow{\mu}\cdot\vec{\omega}) = \overleftrightarrow{\mu}:\overleftrightarrow{\nabla\omega} - \vec{\tau}\cdot\vec{\omega} \qquad\qquad \text{IV.19}$$

$$\frac{\partial\rho u}{\partial t} + \vec{\nabla}\cdot(\rho u\vec{v} + \vec{q}) = -\overleftrightarrow{\tau}:\overleftrightarrow{\nabla v} - \overleftrightarrow{\mu}:\overleftrightarrow{\nabla\omega} + \vec{\tau}\cdot\vec{\omega} \qquad\qquad \text{IV.20}$$

In each expression there is again the convective term representing a reversible flux of each kind of energy and a work term as present in the total energy equation IV.17. In addition to these there are source terms on the RHS of each equation. The source term $\overleftrightarrow{\tau}:\overleftrightarrow{\nabla u}$ represents the Rayleigh dissipation function. Its presence in IV.18 and IV.20 signifies that in a viscous fluid kinetic energy will be dissipated into random thermal energy. Likewise the source term $\overleftrightarrow{\mu}:\overleftrightarrow{\nabla\omega}$ present in IV.19 and IV.20 signifies the dissipation of internal rotational energy into heat by viscous effects.

An unusual feature of fluids with a non-symmetric stress tensor is brought out by the source term $\vec{\tau}\cdot\vec{\omega}$ in equations IV.19 and IV.20. Depending on the sign of the components of the anti-symmetric stress vector $\vec{\tau}$ and the spin vector $\vec{\omega}$ rotational energy can be converted into random thermal energy or vice versa. In other words, in a mixing length fluid internal rotational energy does not necessarily dissipate away, but can be sustained in a steady state from the available random thermal energy.

IV.3   Transport Equations in a Mixing Length Fluid.

In the dynamical equations written in the preceding section the variables outnumber the equations, i.e., they form an indeterminate system. Before solutions for particular situations can be obtained from them a number of additional equations should be obtained which yield a determinate system of equations. Examples of such equations are the kinetic and caloric equations of state relating the pressure and the internal energy to the density and temperature of the fluid, and the transport equations relating the diffusive fluxes of momentum, angular momentum and energy to the parameters of the fluid and their derivatives. We will now follow the standard thermodynamic procedure to derive these transport equations for a fluid possessing spin as an additional degree of freedom (Grad, 1952).

The starting point of the thermodynamic procedure to derive transport equations from the dynamical equations is the first law of thermodynamics, expressing entropy changes as the result of changes in internal energy and reversible work on the system under consideration. For a fluid element undergoing volume changes the first law has the form (deGroot, 1962):

$$T \frac{ds}{dt} = \frac{du}{dt} + \frac{p}{\rho} \vec{\nabla} \cdot \vec{v} \qquad \text{IV.20}$$

where s is the specific entropy of the fluid. In equation IV.20 convective time derivatives are used. The spin forces which we propose in a mixing length fluid cannot do reversible work on a fluid element because the spin field is divergence less $(\vec{\nabla} \cdot \vec{\omega} = 0)$ as follows from equation IV.4. At any rate such a contribution would be without consequence as will be seen in the following discussion.

In line with the second law of thermodynamics we now assume that all irreversible processes in the fluid proceed in such a way as to increase the entropy inside a fluid element, i.e.,

$$\rho \frac{ds}{dt} + \vec{\nabla} \cdot \frac{\vec{q}}{T} \geq 0 \qquad \text{IV.21}$$

where $\vec{q}/T$ represents the diffusive entropy flux. With the aid of equation IV.20 and of the expression for the internal energy IV.20 the condition IV.21 can be expressed as (D'en and Listrov, 1971):

$$-\vec{q} \cdot \vec{\nabla} \frac{1}{T} - \tau \frac{\vec{\nabla} \cdot \vec{v}}{T} - \vec{\tau} \cdot (\vec{\nabla} \times \vec{v} - 2\vec{\omega}) - \overset{o}{\overset{o}{\tau}} : \overset{o}{\nabla} \overset{o}{v}$$

$$-\mu \frac{\vec{\nabla} \cdot \vec{\omega}}{T} - \vec{\mu} \cdot \frac{\vec{\nabla} \times \vec{\omega}}{T} - \overset{o}{\overset{o}{\mu}} : \overset{o}{\nabla} \overset{o}{\omega} \geq 0 \qquad \text{IV.22}$$

In this expression the various tensors and dyadics have been decomposed into their diagonal, antisymmetric and symmetric and traceless parts and the diagonal and antisymmetric parts are represented by their representative scalars and vectors respectively.

56

The inequality IV.21 is to hold for all conceivable non-equilibrium situations. The expression consists of a sum of terms each of which consists of a diffusive flux and its associated thermodynamic force. With linear relations between each flux and its associated force the expression IV.22 can be converted into a positive definite sum of squares.

We will confine ourselves to the simplest case of an isotropic fluid, i.e. one with scalar transport coefficients. In that case fluxes can only depend on forces which have the same transformation properties (Curie's theorem). In this sense the fluxes and forces in equation IV.21 are to be classified as scalar and pseudoscalar ($\tau, \vec{\nabla} \cdot \vec{v}$ resp. $\mu, \vec{\nabla} \cdot \vec{\omega}$), vector and pseudo vector ($\vec{\mu}, \vec{\nabla} \times \vec{\omega}$ resp. $\vec{\tau}, \vec{\nabla} \times \vec{v} - 2\vec{\omega}$) and tensor and pseudotensor ($\overset{\circ}{\underset{=}{\tau}}, \overset{\circ}{\underset{=}{\nabla v}}$ resp. $\overset{\circ}{\underset{=}{\mu}}, \overset{\circ}{\underset{=}{\nabla \omega}}$). According to Curie's theorem, the scalar fluxes can depend in an isotropic system only on scalar forces, vector fluxes only on vector forces, etc. In this way we obtain for the diffusive momentum fluxes:

$$\tau = -\eta_v \vec{\nabla} \cdot \vec{v} \qquad\qquad \text{IV.22a}$$

$$\vec{\tau} = -\eta_r (\vec{\nabla} \times \vec{v} - 2\vec{\omega}) \qquad\qquad \text{IV.22b}$$

$$\overset{\circ}{\underset{=}{\tau}} = -\eta \, \overset{\circ}{\underset{=}{\nabla v}} \qquad\qquad \text{IV.22c}$$

Thus in a fluid with antisymmetric stress tensor and spin there is a third type of viscosity, which may be termed "rotational viscosity" in addition to the regular shear viscosity η and the volume viscosity η_v. Because of the proportionality which we propose between the vorticity $\vec{\nabla} \times \vec{v}$ and the spin $\vec{\omega}$ (equation IV.4) the sign of the vector $\vec{\tau}$ is determined by the magnitude of the proportionality constant ξ :

$$\vec{\tau} = -\eta_r (1 - \frac{1}{\xi}) \, \vec{\nabla} \times \vec{v} \qquad\qquad \text{IV.23}$$

For $\xi < 1$ the vector $\vec{\tau}$ has the opposite sign as for $\xi > 1$. This means in turn that the magnitude of ξ determines the way in which the spin-orbit coupling in equations IV.14 and IV.15 takes place and whether random thermal energy will be converted into rotational energy or vice versa according to equations IV.19 and IV.20.

According to the Curie theorem a linear coupling can exist between the diffusive fluxes of energy and angular momentum in isotropic fluids subject to the inequality equation IV.22. In that case there is a contribution to the heat flux proportional to the curl of the spin field and a contribution to the diffusive angular momentum flux proportional to the gradient of the temperature field. Onsager has shown that in the framework of kinetic theory the proportionality factors for such cross effects are closely related to each other in a way depending on the nature of the thermodynamic forces. These relations ultimately stem from the time-symmetry of the equations of motion for molecules on the microscopic level. As a further requirement for the validity of the Onsager relations the deviations from thermodynamic equilibrium should be small. The mixing length theory of convective heat transport is an attempt to describe turbulent convection in terms of the kinetic theory. The convective parcels form the "molecules" of the mixing length fluid and the mixing length represents the mean free path of each parcel. Also the equations of motion for individual parcels possess time-symmetry: their motion is described by the balance of buoyancy and inertia, to the exclusion of dissipative forces which would destroy the time-symmetry of the equations of motion.

One fundamental difference between ordinary fluids and a mixing length fluid is in the condition of equilibrium. In ordinary fluids there is no dissipation in the equilibrium state, but in mixing length fluids a dissipative heat flux is indispensable for the maintenance of the state of convective equilibrium. This is a serious objection against the use of linear transport equations and the Onsager relations. On the other hand, such attempts as have been made to describe the dynamics of mixing length fluids have all used linear transport equations for the momentum, with the molecular viscosity replaced by a hypothetical "eddy viscosity."

From equation IV.22 the linear transport equations for heat and angular momentum must have the form (D'en and Listrov, 1971):

$$\vec{q} = -\kappa \vec{\nabla} T + \beta T \vec{\nabla} \times \vec{\omega} \qquad \text{IV.24}$$

$$\vec{\mu} = \beta \vec{\nabla} T + \gamma \vec{\nabla} \times \omega \qquad \text{IV.25}$$

58

Here we have used the Onsager principle that the same coupling constant β connects the heatflux to the spin field and the angular momentum flux to the temperature field. The meaning of the condition IV.8 on the couple stress tensor now becomes clear: for a symmetric couple stress tensor the vector $\vec{\mu}$ representing the antisymmetric part of the couple stress tensor must vanish. If there is no thermomechanical effect ($\beta = 0$) then by equation IV.25 the curl of the spin field must also vanish. This means that in a fluid with symmetric couple stresses and without thermomechanical effect no closed vortex lines can exist. On the other hand, if there is a significant thermomechanical effect, no heat flux can take place without the formation of vortex rings. The contribution of these vortex rings to the heat flux is then parallel to the temperature gradient.

According to equation IV.24 there are two contributions to the heat flux in a mixing length fluid. The first, proportional to the temperature gradient as in Fourier's law, represents the heat transfer by the vertical translatory motions of convective parcels. In the mixing length picture the vertical motions take place adiabatically and reversible, and they are followed by an isobaric thermalization of the temperature difference which has developed between the parcels and the ambient fluid. An individual parcel operating between two levels thus performs a thermodynamic cycle consisting of two isentropics and two isobarics. The area enclosed by this cycle will represent the amount of work which is done on the environment. This work will go into kinetic energy of the surrounding medium.

The second term of equation IV.24 represents the contribution of internal rotations to the heat flux. From the geometrical meaning of the curl operator the interpretation of the rotatory heat flux is as follows: the rotation of individual parcels can be accompanied by a ring current of heat. The strength of these ring currents may be taken to be proportional to the spin of each parcel. The net heat transfer by a volume distribution of spins is given by the curl of the spin field, as in equation IV.24. The relative significance of the rotational heat flux has not been evaluated quantitatively for reasons given in connection with equations III.2.

If a thermomechanical effect is to occur according to equations IV.24 and IV.25 then the internal rotations must be accompanied by ring currents of heat. We propose that such is the case in the presence of partial ionization, but not for full ionization, for the following reason: the internal

energy of a fully ionized plasma consists entirely of random thermal motion
of the electrons and atoms; in other words, the amount of internal energy
is completely determined by the pressure. During an isobaric rotation the
distribution of internal energy of a parcel does not change and no energy
transfer takes place. This does not hold when the internal energy distri-
bution of a parcel depends on other variables besides the pressure, as is
the case in the presence of partial ionization. For, during an isobaric
rotation of a parcel with a superadiatic temperature gradient in which the
pressure surfaces remain horizontal, the temperature and density surfaces
will become tilted in opposite fashions. If the rotation of the parcel is
approximately uniform, the degree of ionization in the parcel has to adjust
itself in a manner which brings about a ring current of heat in the plane
of the rotation.

IV.4 Application to the Solar Convection Zone.

After the substitution of the transport equations into the dynamical
equations for mixing length fluids as obtained in sections IV.2 and IV.3
there are two traditional ways of obtaining a determinate system of equa-
tions describing the flow pattern. In the simplest method a relation be-
tween the pressure and density of the fluid is assumed. In that case the
continuity equation and the momentum balance form a set of four equations
with four unknowns, namely the three components of the velocity and either
the density or the pressure. This is called the barotropic description of
a fluid. It ignores all thermal effects and thereby achieves only a par-
tial description of the fluid.

A more realistic description results if the kinetic equation of state
relates the pressure to both the density and the temperature. In this case
the caloric equation of state is necessary to arrive at a closed set of
equations. One obtains a description of the temperature field as well as
the flow pattern. This description is termed the baroclinic description
of the fluid.

The earliest attempts at a fluid dynamical description of the solar
rotation were made in the barotropic framework by assuming an adiabatic
relationship between the pressure and the density of the solar convection

60

zone. It was ascertained from mixing length theory that this would be a good approximation in fully ionized convective layers. It was assumed that the preferential direction of gravity would affect the turbulent momentum exchange. This proposed effect was described with an anisotropic viscosity through a parameter s whose magnitude determined whether the radial momentum exchange should be enhanced or inhibited. It was found that in order to get equatorial acceleration the radial momentum exchange should be diminished in radial directions. In that case a meridional circulation would be set up rising at the poles and sinking at the equator which would sustain the equatorial acceleration.

Returning to our dynamical equations for the convection zone we can put the viscous forces in the momentum equation in the form:

$$\vec{\nabla} \cdot \overset{\leftrightarrow}{\tau} = -\eta \nabla^2 \vec{v} - (\frac{1}{3}\eta + \eta_v) \vec{\nabla}(\vec{\nabla} \cdot \vec{v}) - \eta_r (\frac{1}{\xi} - 1) c\vec{q} \qquad \text{IV.25}$$

where the transport equations IV.22, IV.23, IV.24, and the relation IV.4 have been used. The transport coefficients have been assumed constant. The first term on the RHS represents the familiar viscous force due to shear, as in the Navier-Stokes equation. The second term stands for the viscous forces due to expansion or contraction of fluid volumes. The third term is a new term due to presence of antisymmetric stresses and to the difference between spin and vorticity. In the solar convection zone with its radial heat flux it will affect the radial flux of momentum. The effect will be such that for $\xi < 1$ the radial momentum flux is enhanced, for $\xi > 1$ the radial momentum flux is diminished. This means that the parameter ξ describing the relation between spin and vorticity has the same function as the parameter s describing the anisotropy of the viscosity tensor. For a positive meridional circulation to occur we must have $\xi > 1$, which corresponds to a predominance of hot, rising parcels in the solar convection zone, as was shown in section IV.1.

In the baroclinic description the attention focuses on the properties of the heat conductivity, in particular on its possible latitude dependence. Such a latitude dependence has been proposed as the cause of the equatorial acceleration of the sun. At the solar equator the rotation is thought to affect the convective heat transport. This would cause a temperature

difference to develop between the equator and the poles. In such a baro-
clinic situation a meridional circulation would develop which would counter-
act the effect of rotation on the convective heat transport. This merid-
ional circulation would again be responsible for the equatorial accelera-
tion.

According to the formalism of section IV.3 and the condition IV.4 the
heat flux and the temperature gradient in mixing length fluids are related
by

$$\vec{q} = -(\kappa + \frac{\beta^2 T}{\gamma}) \vec{\nabla} T \qquad \qquad IV.26$$

This means that the effective heat conductivity in layers with a thermo-
mechanical effect β is enhanced by a factor $\beta^2 T/\gamma$. On the sun this
effective heat conductivity shows no observable latitude-dependence. The
interpretation of equation IV.26 then is that the terms κ and β sepa-
rately contain latitude dependences which cancel in the effective heat con-
ductivity. In other words, the meridional circulation exactly compensates
for any temperate difference between equator and pole which arises from the
effect of rotation on convective heat transfer.

An alternative formulation is obtained by eliminating $\vec{\nabla}T$ from equa-
tion IV.22 and IV.23 through the condition IV.7. With equation IV.4 one ob-
tains a direct relationship between the velocity field and the heat flux
in the form

$$\vec{\nabla} \times \vec{\nabla} \times \vec{v} = c\vec{q} \qquad \qquad IV.27a$$

$$c = \frac{2\xi\beta}{\kappa\gamma + \beta^2 T} \qquad \qquad IV.27b$$

If the form of the heat flux is known, equation IV.27a leads directly
to the associated flow pattern provided that the dependence of the thermo-
mechanical effect on position be known. In practical cases a high degree
of symmetry and a simple position dependence of c will be required for
obtaining analytic solutions of IV.27. It appears that in the solar con-
vection zone both of these conditions are met to a sufficient degree for

equation IV.27a to yield useful analytical results for the thermally driven

flows in the solar convection zone.

V GLOBAL SOLUTIONS

In the previous chapter we have derived an equation connecting the
velocity field to the convective heat flux in a mixing length fluid. Ac-
cording to this equation, the vorticity of a mixing length fluid acts as
the vector potential of the convective heat flux. Alternatively, the heat
flux is the source term for three coupled second order partial differential
equations for the velocity. The integration of these equations for a given
heat flux and boundary conditions leads to the admissible flow pattern of
that situation.

For the solar convection zone two cases with analytic forms for the
convective heat flux and for the boundary conditions on the velocity field
present themselves. Taken as a whole the convection zone is a spherical
shell with uniform temperature distribution at the outer surface. Below
the surface there is a purely radial heat flux following the inverse square
law. In addition, admissible flow patterns in the convection zone have to
meet the observed surface motion. The resulting flow patterns for the con-
vection zone as a whole we term the global solutions of our equation for
convective heat transfer. These are concerned with the equatorial accel-
eration and meridional circulation of the sun. It is also possible to con-
sider a part of the convection zone small enough that its curvature can be
neglected, but large enough that mixing length theory is still applicable.
In such regions a uniform surface temperature distribution is the result
of a uniform heat flux underneath. The admissible flow patterns for this
type of heat flux we term the local solutions. They pertain to the Evershed-
flow and to the supergranulation.

In solving the equation IV.27a for a given heat flux and boundary con-
ditions the analogy with the equations for magnetic media is quite helpful,
particularly because the spherical shell and the cylinder are standard
problems in magnetostatics. The well-known techniques of integration

through separation of variables, through Stokes' theorem or through Green's functions lead directly to analytic representations of the flow patterns in the solar convection zone.

Before solving equation IV.27a for the convection zone as a whole we want to outline the rotational history of the sun in the framework of stellar evolution as presently understood. We envisage that the sun originated from a gas cloud with fairly uniform mass distribution and with a fairly uniform intrinsic rotation, i.e. a fairly uniform field of vortex lines. As this gas cloud contracted, every volume element conserved its orbital angular momentum, because the low density made viscous effects negligible. In other words, the vortex lines were frozen into the gas, and the regions with the highest mass density also obtained the highest concentration of vortex lines. In this way the central regions of the collapsing cloud acquired the highest rotation rate. With the onset of convection in the Hayashi phase the material ceases to behave as a frictionless fluid. From then on orbital angular momentum of fluid elements is no longer conserved; or, equivalently, the vortex lines are partially decoupled from the stellar material.

The present theory claims that the vortex lines in the convective region redistribute themselves in a manner depending on the presence or absence of partial ionization in the convective material. As discussed in Chapter IV, in fully ionized convective regions no closed vortex lines can be formed. By contrast, the formation of vortex rings in regions with significant partial ionization is compulsory. Since the bulk of the convective envelope will be fully ionized, we first investigate what rotation pattern will evolve after the onset of convective equilibrium in which all vortex lines remain open.

V.1   Without Thermomechanical Effect.

According to the present theory, the rotational state of a mixing length fluid has to be described by two different vector fields. In addition to the vorticity field specifying the rotational motion of an ensemble

of convective parcels, there is the spinfield specifying the rotational motion of convective parcels about their center of mass. From its definition as the curl of the velocity field it follows that the vorticity is divergenceless. For the fully ionized mixing length fluid which we are presently considering it follows from equation IV.27a that the curl of the spinfield must vanish; this condition states mathematically that there can be no closed vortex lines in a fluid without thermomechanical effect. Thus we have for the vorticity field $\vec{w}$ and the spin field $\vec{\omega}$

$$\vec{\nabla} \cdot \vec{w} = 0 \tag{1a}$$

$$\vec{\nabla} \times \vec{\omega} = 0 \tag{1b}$$

In Chapter IV we have argued that the vorticity and spin fields in a mixing length fluid are not independent of each other. Rather, they are connected by a scalar coefficient ξ which remains close to unity throughout the mixing length fluid. With regard to the behavior of vortex lines after convection sets in, the presence of a convective envelope is equivalent to a region in which the parameter ξ is different but close to unity. Outside this region ξ remains exactly one. Taking the outer radius of the convective shell at $r = 1$ and the inner radius at $r = X$ we can summarize the above relations between the vorticity and spin fields in the following form:

$$\vec{w} = 2 \, \xi^{(i)} \vec{\omega} \tag{2a}$$

$$\xi^{(i)} = \begin{cases} 1 & r < X \\ \xi & X < r < 1 \\ 1 & r > 1 \end{cases} \tag{2b}$$

In equation (2a) we have introduced a factor 2 because one-half of the vorticity rather than the vorticity itself represents a rotation rate.

The equations (1,2) describe the rotational state of a convective envelope in complete analogy with the equations for the electrical state of a

dielectric shell in an external electric field and with the magnetic state of a permeable shell in an external magnetic field. For the solution two alternatives present themselves. Equation (1b) implies that the spinfield everywhere has a scalar potential, which by equations (1a,2) must obey Laplace's equation. On the other hand, equation (1a) implies that the vorticity has a vector potential, which is of course the velocity. For our present purposes it is more convenient to use the vector potential method to solve equations (1,2) since this leads directly to the velocity field.

For the solution of equations (1,2) we introduce a right-handed spherical coordinate system with the origin at the center of the star and the polar axis along the axis of rotation. We impose axial symmetry, so that all φ-derivatives vanish. In addition, the star is in a steady state in which the inner and outer radius of the convective envelope remain constant. This means that there are no radial or meridional velocities, for in combination with the axial symmetry any such meridional circulation would constitute a vortex ring, which is prohibited by equations (1b,2). Thus we are only concerned with the azimuthal component of the velocity. The second order partial differential equation which the azimuthal velocity v_φ obeys according to equations (1,2) can be solved immediately by separation of variables in spherical coordinates r, θ, φ. Taking into account the azimuthal symmetry, the differential equation for the azimuthal velocity and its solution are respectively:

$$\left[\frac{\partial}{\partial r} \, r^2 \, \frac{\partial}{\partial r} + \frac{1}{\sin\theta} \frac{\partial}{\partial\theta} \sin\theta \frac{\partial}{\partial\theta} - \frac{1}{\sin^2\theta} \right] v_\varphi = 0 \qquad (3a)$$

$$v_\varphi = \sum_{\ell=1}^{\infty} \left(A_\ell r^\ell + \frac{B_\ell}{r^{\ell+1}} \right) P_\ell^1 (\cos\theta) \qquad (3b)$$

The solution (3b) represents a sum of two types of modes whose radial dependence completely determines their latitude-dependence and vice-versa. The first type of mode, $A_\ell r^\ell P_\ell^1(\cos\theta)$, diverges for large values of r, the second type, $\frac{B_\ell}{r^{\ell+1}} P_\ell^1(\cos\theta)$ has singularities at the origin. In both cases the singularity is stronger for the higher modes. In connection with the oscillatory nature of the associated Legendre-polynomials, the azimuthal

velocity will follow the sign changes of the highest mode in the neighborhood of each singularity. Only the lowest mode of each type, $\ell = 1$, is exempt of this oscillatory behavior.

The equation (3a) and the general form of its solution (3b) apply in all three regions which were defined in equation (2b). We denote these three regions as the core, the envelope and the atmosphere of the star. It is convenient to write the solutions (3b) in these three regions in terms of the angular velocity $\Omega = v_\varphi / r \sin\theta$, viz:

$$\Omega^{(i)} = \sum_{\ell=1}^{\infty} \left(A_\ell^{(i)} r^{\ell-1} + \frac{B_\ell^{(i)}}{r^{\ell+2}} \right) \frac{P_\ell^1(\cos\theta)}{\sin\theta} \tag{4a}$$

$$
\begin{aligned}
i = 1 &: \quad r < X \quad\quad\; , \text{ Core} \\
i = 2 &: \quad X < r < 1 \;, \text{ Envelope} \\
i = 3 &: \quad r > 1 \quad\quad\;\; , \text{ Atmosphere}
\end{aligned}
\tag{4b}
$$

At the interfaces of the three regions (4b) boundary conditions following from equations (1) are to be met. At each interface the perpendicular component of the vorticity and the tangential component of the spin have to be continuous, regardless of the discontinuity in ξ which equation (2b) defines there. In terms of the orbital angular velocity Ω, these boundary conditions take the form:

$$\text{at } r = X: \quad \Omega^{(1)} = \Omega^{(2)}, \quad \frac{\partial}{\partial r}[r^2\Omega^{(1)}] = \frac{1}{\xi}\frac{\partial}{\partial r}[r^2\Omega^{(2)}] \tag{5a}$$

$$\text{at } r = 1: \quad \Omega^{(2)} = \Omega^{(3)}, \quad \frac{1}{\xi}\frac{\partial}{\partial r}[r^2\Omega^{(2)}] = \frac{\partial}{\partial r}[r^2\Omega^{(3)}] \tag{5b}$$

The first of the conditions (5a,b) implies that there are no discontinuities in the angular velocity at surfaces where the parameter ξ changes discontinuously, i.e. at the interface of a convective and a non-convective region. The second of the conditions (5a,b) implies that at such interfaces the radial angular velocity gradient will generally suffer a discontinuity.

After substitution of the solutions (3a) in the boundary conditions (5a,b) one obtains a system of four linear equations connecting the six coefficients specifying each individual order. In general a fifth equation

will be provided by the observational knowledge of the rotation at the outer surface of the star. This leaves the system of equations for the coefficients $A_{\ell}^{(1)}$, $B_{\ell}^{(1)}$ still indeterminate. We will therefore specify to two extreme types of solution, namely one type representing a star with a rapidly rotating core and another appropriate for a slowly rotating interior.

A slowly rotating interior corresponds to the absence of divergent terms in the solution (4a) pertaining to the core, i.e. $B_{\ell}^{(1)} = 0$. In this case the boundary conditions (5) can only be satisfied if both types of mode survive in the atmospheric solution. The $\ell = 1$ order then corresponds to a constant rotation rate at infinity; all higher orders bring about divergences in the angular velocity at infinity. The alternative is to assume a fast core and vanishing angular velocities at large distances, i.e. $A_{\ell}^{(3)} = 0$. In our introduction to this chapter we have opted for this case by arguing that the stellar regions with the highest mass density also acquire the highest angular velocity.

The rotation pattern not only depends on the relative values of the coefficients of a given mode, but also on the relative importance of the modes of different order. Only the $\ell = 1$ order has no latitude dependence, all the higher orders have a latitude dependence with an oscillatory character. In the neighborhood of the singularities this oscillatory character leads inevitably to sign changes in the azimuthal velocity. On physical grounds we want to rule out such sign changes, either at large distances for the slow core case or near the center for the rapid core case. This restricts solution (4a) to the lowest order mode $\ell = 1$. The solution for all three regions then has the form
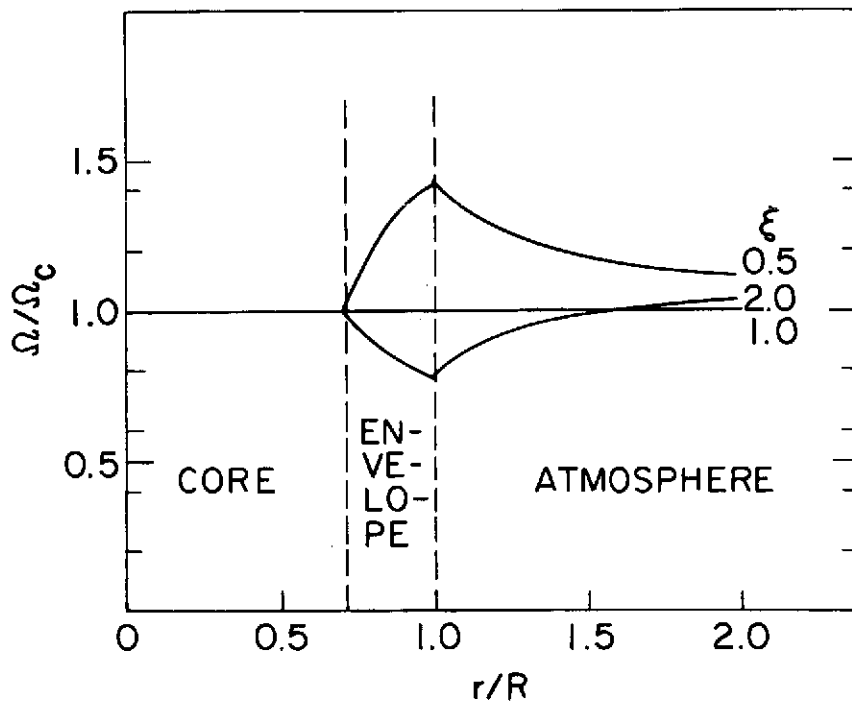
$$\Omega^{(i)} = A^{(i)} + B^{(i)}/r^3 \tag{6}$$

where the coefficients $A^{(i)}$, $B^{(i)}$ appropriate to the two cases are given in Table 1.
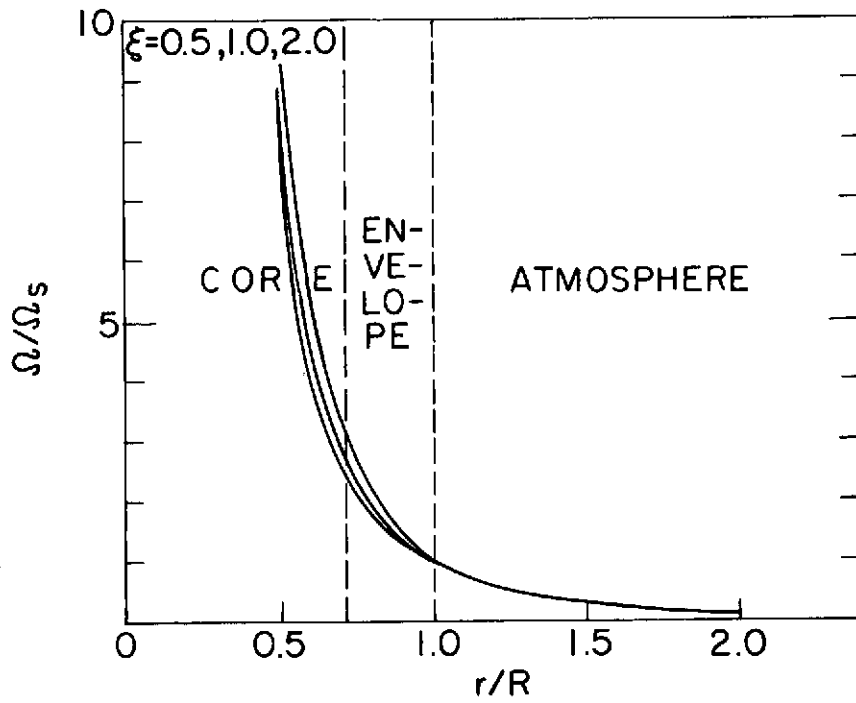
(a) Rapid core

(b) Slow core

Figure 4. Rotation patterns obtained for different
boundary conditions and values of the
spin parameter.

70

Table 2

EXPRESSIONS FOR THE COEFFICIENTS OF
THE SOLUTION (6) IN TERMS OF THE PARAMETER ξ AND
THE THICKNESS OF THE CONVECTIVE ENVELOPE

Region	$A^{(i)}$	$B^{(i)}$
Slow Core Core	1	0
Envelope	$\dfrac{2\xi + 1}{3}$	$-\dfrac{2(\xi-1)x^3}{3}$
Atmosphere	$\dfrac{(2\xi+1)(\xi+2) - 2(\xi-1)^2x^3}{9\xi}$	$\dfrac{2(2\xi+1)(\xi-1)(1-x^3)}{9\xi}$
Rapid Core Core	$\dfrac{(\xi+2)(\xi-1)(1-x^3)}{9\xi x^3}$	$\dfrac{(2\xi+1)(\xi+2) - 2(\xi-1)^2x^3}{9\xi}$
Envelope	$-\dfrac{\xi - 1}{3}$	$\dfrac{\xi + 2}{3}$
Atmosphere	0	1

The rotation patterns described by equation (6) with the coefficients
as in Table 1 contain two adjustable parameters. Of these, X expresses
the thickness of the convective envelope. The value of X depends on the
evolutionary stage of a star in a manner which can be calculated from the
theory of stellar structure. For the present sun, the value adopted by
Baker and Temesvary is .713, corresponding to a convective shell with a
thickness of 200,000 km. This value has been used in the graphs 4a and b,
showing the dependence of the angular velocity and radius for the two cases
and for different values of the parameter ξ.

Figure 4b shows that with a slow core the cases $\xi \gtrless 1$ make a critical
difference; in either case the radial velocity gradients have opposite
signs outside the core, and the angular velocity reaches a maximum resp.
a minimum on the outer surface. As ξ goes to unity, the rotation pattern
passes into uniform rotation everywhere. In the case of the rapid core

the variation of ξ within its limits does not make much difference. The general pattern follows a $1/r^3$ dependence on radius. This law is followed more and more closely as ξ approaches unity (Figure 4a).

V.2 With Thermomechanical Effect.

The discussion in the previous section was restricted to those parts of the convection zone in which partial ionization is negligible. In practice we mean by this that both hydrogen and helium are fully ionized. On the sun this is the case in the lower 80% of the convection zone model given by Baker and Temesvary. At about 35,000 km below the surface helium begins to de-ionize, and at about 7,000 km below the surface the first neutral hydrogen atoms appear. Both elements are effectively neutral at the solar surface. With a solar radius of 700,000 km, we will therefore adopt for the region of partial ionization of helium the top 5% of the solar layers, and for the region of partial ionization of hydrogen the top 1% of the solar layers.

According to the present theory, the behavior of mixing length fluids depends critically on the absence or presence of a significant partial ionization. As explained in Chapter IV, the partial ionization is responsible for the formation of closed vortex lines. On a global scale such vortex rings constitute a meridional circulation, which in combination with an external rotation lead to equatorial acceleration of the partially ionized layers. In the following sections we will derive solutions for the azimuthal vorticity and velocity of a spherical shell with constant thermomechanical effect. In order to match the boundary conditions at the inside and the outside of the shell it will be necessary to introduce surface currents of heat at each of these boundaries. These current sheets form an alternative complete description of the rotational state of a mixing length fluid with significant partial ionization.

V.2.1 Meridional Circulation.

In a layer with a significant partial ionization the equation for convective heat transfer can be written as:

$$\vec{\nabla} \times \vec{w} = c\vec{q} \tag{7a}$$

$$c = \frac{2\xi\beta}{\kappa\gamma + \beta^2 T} \tag{7b}$$

where β is the thermomechanical effect. Before equation (7a) can be integrated, the dependence on position of the term $c\vec{q}$ has to be found. For this purpose we note that by equation (7a) the divergence of $c\vec{q}$ has to vanish. According to the discussion of Chapter IV, there are no sources or sinks of heat in the entire convection zone; in other words, the divergence of the heat flux has to vanish also. For a spherical shell with uniform temperature distribution at the surface this means that the radial heat flux follows the inverse square dependence on distance from the center. In addition, the coefficient c in equation (7) cannot depend on radius in the region where the divergence of both $c\vec{q}$ and $\vec{q}$ vanishes. Thus we have:

$$q_r = \frac{L_\odot}{4\pi r^2} \tag{8a}$$

$$c(r) = \begin{cases} 0 & r < Y \\ c & Y < r < 1 \\ 0 & r > 1 \end{cases} \tag{8b}$$

where $L_\odot$ is the solar luminosity. The outer radius of the convection zones has again been taken as unity, and the inner boundary of the region with significant partial ionization is at $r = Y$. The boundaries of this region are thus characterized by discontinuities in the coefficient c and, equivalently, in the thermomechanical effect β.

With the forms (8a,b) for the inhomogeneous term, equation (7a) can now be integrated using Stokes' theorem. For this purpose a circular loop centered on the rotation axis is to be taken, where the loop bounds a section of a spherical surface concentric with the origin. If the loop lies inside the shell with thermomechanical effect, i.e. between radii Y and 1 then a non-vanishing surface integral of the heat flux implies a non-vanishing line integral of the azimuthal velocity, or:

73

$$\frac{1}{r \sin\theta} \frac{\partial}{\partial \theta} (\sin\theta \, w_\varphi) = \frac{cL_\odot}{4\pi r^2} \qquad (9a)$$

$$w_\varphi = \frac{cL_\odot}{4\pi} \frac{\pm 1 - \cos\theta}{r \sin\theta} \qquad (9b)$$

In equation (9b) the plus-sign (+) applies to the northern hemisphere and the minus-sign (−) to the southern hemisphere.

The azimuthal vorticity given by equation (9b) constitutes a meridional circulation which for positive c rises at the poles and sinks at the equator. The discontinuities in c at the boundaries of the shell are responsible for similar discontinuities in w_φ at those locations. In addition, the azimuthal vorticity changes sign discontinuously in the equatorial plane of the shell. All these discontinuities are accompanied by surface currents of heat, which we will now proceed to calculate.

According to equation (7a) a discontinuity in the tangential vorticity across a surface has to be matched by a surface current of heat of the appropriate magnitude and direction. The direction of such a current sheet has to be perpendicular to the discontinuous component of the vorticity. At the boundaries of the shell this means that the surface current is meridional, but in the equatorial plane it has to be radial. For both cases we find:

$$\text{at } r = Y: \quad q_{s\theta} = -\frac{L_\odot}{4\pi Y} \frac{\pm 1 - \cos\theta}{\sin\theta} \qquad (10a)$$

$$\text{at } r = 1: \quad q_{s\theta} = \frac{L_\odot}{4\pi} \frac{\pm 1 - \cos\theta}{\sin\theta} \qquad (10b)$$

$$\text{at } \theta = \frac{\pi}{2}: \quad q_{sr} = -\frac{L_\odot}{4\pi} \frac{1}{r} \qquad (10c)$$

Thus the entire shell with thermomechanical effect is surrounded and divided in half by surface currents of heat. It is these current sheets which enable only the small region where partial ionization is significant to have a meridional circulation, whereas in the rest of the convection zone and elsewhere the azimuthal vorticity remains zero and the simple rotation patterns derived in the previous section remain valid.

The nature of the meridional circulation becomes more clear by investigating the stream function of the solution given by equation (9b). In view of the assumed axial symmetry, the radial and meridional components of the velocity can be expressed in terms of Stokes' stream function in such a way that they obey the continuity equation identically. The streamlines of the flow are then given by the condition that the stream function is a constant. In the present spherical coordinates, the continuity equation and its solution in terms of the Stokes' stream function take the form:

$$\frac{1}{r^2} \frac{\partial}{\partial r} (r^2 \rho v_r) + \frac{1}{r \sin\theta} \frac{\partial}{\partial \theta} (\sin\theta \, \rho v_\theta) = 0 \qquad (10'a)$$

$$v_r = \frac{-1}{\rho r^2 \sin\theta} \frac{\partial \psi}{\partial \theta} \;, \quad v_\theta = \frac{1}{\rho r \sin\theta} \frac{\partial \psi}{\partial r} \qquad (10'b)$$

where ρ represents the mass density of the fluid. As discussed in Chapter III, for the sun ρ may be taken independent of latitude, but having a strong dependence on radius.

The stream function ψ obeys a second order partial differential equation which can be found by substituting equation (10'b) for the radial and meridional velocity components into equation (9b) for the azimuthal vorticity. The boundary conditions on ψ are to reflect the presence of a rigid inner surface and a free outer surface of the shell with merdional circulation. That is, on the inner boundary both the radial and the meridional component of the velocity vanish, but on the outer surface only the radial velocity is assumed to vanish. The rigid inner boundary derives from the circumstances that in the layers below the shell with thermomechanical effect no meridional circulation can exist and that no slip is allowed at the interface of these regions. The free surface at the outer boundary is justified by the sharp outward decrease in density which makes the dynamical effect of the atmospheric layers on the convective layers negligible. Considering equation (10'b) and assuming the stream function separable in r and θ the above considerations impose that the stream function vanishes on both surfaces and has a vanishing normal derivative on the inner surface of the shell with meridional circulation. The stream function is then determined by the system:

$$\left[\frac{\partial}{\partial r}\frac{1}{\rho}\frac{\partial}{\partial r} + \frac{\sin\theta}{r^2}\frac{\partial}{\partial\theta}\frac{1}{\rho\sin\theta}\frac{\partial}{\partial\theta}\right]\psi = \frac{cL_\odot}{4\pi}(\pm 1-\cos\theta) \qquad (10''a)$$

$$\text{at } r = Y : \quad \psi = 0 \ , \ \frac{\partial\psi}{\partial r} = 0 \qquad\qquad (10''b)$$

$$\text{at } r = 1 : \quad \psi = 0 \qquad\qquad (10''c)$$

The second order partial differential equation (10''a) is of the ellip-
tic type. Such equations have unique, stable solutions in closed regions
with Dirichlet- or Neumann-type boundary conditions. In other words, for
equation (10''a) to have a unique, stable solution inside the shell with
meridional circulation, either the values of ψ or its normal derivative must
be known over the whole boundary surface. However, in the present case,
according to equations (10''b,c) both the value of ψ and of its normal deriv-
ative are specified over the boundary surface. In other words, we are con-
fronted with an elliptic differential equation for the stream function sub-
ject to Cauchy-type boundary conditions. Such systems do not allow unique,
stable solutions. The solutions of such systems are unstable in the sense
that an infinitesimal change in the boundary conditions leads to an infinite
change in the solution elsewhere. The implication is that the meridional
circulation of the sun can only have a non-steady character, which strictly
speaking, cannot be described by the time-independent formalism which we
have developed in Chapter IV.

The unsteady nature of the equatorial acceleration as evident from the
large fluctuations in observed surface rotation rates was noted in Chapter
II. The foregoing discussion traces back this unsteadiness to the unsteady
nature of the angular momentum transfer from polar to equatorial regions by
the meridional circulation. It may be expected that the solution (9b) ap-
proximates the average meridional circulation over periods long compared to
its fluctuations.

V.2.2 Equatorial Acceleration.

In the previous sections we derived a series-expansion for the angular velocity distribution of a star possessing a convective envelope. We argued that only the lowest order term would survive, i.e. the one without latitude dependence. This is of course at variance the rotation pattern observed on the solar surface, where the equator is found to rotate about 20% faster than the poles. In the present theory as with several earlier ones the cause of this "equatorial acceleration" is sought in the presence of a global meridional circulation as described in the previous section. When rising at the poles and sinking at the equator, this circulation transports angular momentum towards the equatorial regions. This results in a small latitude-dependence superposed on the overall radial dependence of the angular velocity. We will now proceed to investigate the analytic form of this latitude-dependence in the framework of the present theory.

In the first place, we claim that the differential equation (3a) for the azimuthal velocity remains valid even if internal rotations contribute significantly to the total heat flux. The reason for this is that the internal rotations cannot be expected to set up an azimuthal heat flux; this is contrary to the principle of lowest entropy production which we have adopted for the description of the convection zone. By this principle, the rotation pattern is such that the φ-component of the curl of the spin field vanishes. This is equivalent to equation (3a) for the azimuthal velocity. The principle of lowest entropy production does not rule out azimuthal surface currents of heat at the boundaries of the region with thermomechanical effect. Indeed, such current sheets are essential for meeting the boundary conditions on the vorticity and spin fields at these boundaries. Because of the infinitesimal volume occupied by these current sheets, they contribute negligibly to the total dissipation in the convection zone. Restricting ourselves for the moment to within the convective region with thermomechanical effect we have:

$$q_\varphi = 0 \tag{11a}$$

$$\Omega = \sum_{\ell=1}^{\infty} \left(A_\ell r^{\ell-1} + \frac{B_\ell}{r^{\ell+2}} \right) \frac{P_\ell^1(\cos\theta)}{\sin\theta} \quad \left. \right\} \quad Y < r < 1 \tag{11b}$$

77

where P_ℓ^1 $(\cos\theta)$ is the first associated Legendre polynomial. Because of the narrow region below unity to which r is restricted many orders of the expansion (11b) can be used before the difficulties with sign changes mentioned in V.1.1 come into play.

On formulating the boundary conditions on the angular velocity representation (11b) the possible presence of surface currents of heat make for a crucial difference with the case discussed in V.1.1. If there is no thermomechanical effect, then the orbital angular velocity is continuous at the boundary, and the radial derivative suffers a discontinuity at the interface of a convective and a non-convective region. With series expansions for the angular velocity of the form (11b) subject to these conditions, it follows that on either side of the boundary modes of the same order have to be present. In other words, without thermomechanical effect it is not possible to have latitude-dependent terms in one region and not in an adjacent region. On these grounds we restricted our solution for the convective envelope in V.1.1 to the lowest order mode, thereby admitting only radial differential rotation in all three regions of a convective star.

The situation changes drastically if surface currents of heat are allowed on the interface of two regions with vanishing and non-vanishing thermomechanical effect respectively. In that case the different orders of the series (11b) can terminate on the boundary on a current sheet of the proper magnitude and direction. Thus it becomes possible to have a thin shell having latitude-dependent modes sandwiched in between layers where only the lowest order mode exists. On the one hand the surface currents give greater freedom to the rotation pattern of shells with heat-carrying internal rotations; on the other hand, we lose one condition from which this rotation pattern may be derived from the rotation outside such a region.

The condition that the angular velocity itself be continuous is unaffected by the presence or absence of surface currents of heat at the interface of heat or non-heat carrying internal rotations. Even without this condition, we can apply our observational knowledge of the sun's surface rotation to the determination of the constants in equation (11b) because the motions of quiescent prominences and sunspots certainly reflect the

rotation of those layers of the sun where convection is still in full swing. Lacking any direct observations on the rotation of the inner boundary of the shell with thermomechanical effect, we will invoke the continuity of the angular velocity across this boundary and prescribe a latitude-independent rotation at this surface in conformity with the solutions obtained for the fully ionized convection zone in V.1.1. Thus we have:

$$\text{at } r = Y: \quad \sum_{\ell=1}^{\infty} \left(A_\ell Y^{\ell-1} + \frac{B_\ell}{Y^{\ell+2}} \right) \frac{P_\ell^1(\cos\theta)}{\sin\theta} = \Omega_i \qquad (12a)$$

$$\text{at } r = 1: \quad \sum_{\ell=1}^{\infty} (A_\ell + B_\ell) \frac{P_\ell^1(\cos\theta)}{\sin\theta} = \sum_{m=1}^{\infty} \Omega_m \cos^m\theta \qquad (12B)$$

The various values for the constants Ω_0, Ω_1, etc. as observed in different markers on the solar surface are given in Chapter II. The measurements yield only Ω_0, Ω_2 and Ω_4; uneven and higher order terms are below the present limits of detectability.

Since the equations (12a,b) are to hold for all latitudes, each of them constitutes an infinite number of linear equations between the unknown coefficients A_ℓ, B_ℓ and the known coefficients Ω_m. The solution of these equations for each given order ℓ can be obtained by multiplying both sides of equations (12) by $\sin\theta P_\ell^1(\cos\theta)$ and integrating over the surface of the unit sphere. With orthogonality properties of the associated Legendre polynomials two linear equations for the coefficients of a given order ℓ then appear which can be solved immediately. The result of this procedure is given in Table 2. This table only contains those orders which are actually observed on the sun. The latitude-dependent factor of each order is normalized to have the value unity at the poles; its values do not exceed the range ±1. Similarly, the radius-dependent factors of the latitude-dependent modes have been normalized to unity on the outer surface; on the inner surface they vanish in conformity with equation (12a). The radius-dependent factors of the lowest order mode have also been normalized to values between zero and unity between the respective surfaces.

The solution given in Table 2 contains two as yet undetermined parameters, namely the relative inner radius of the shell Y and the rotation
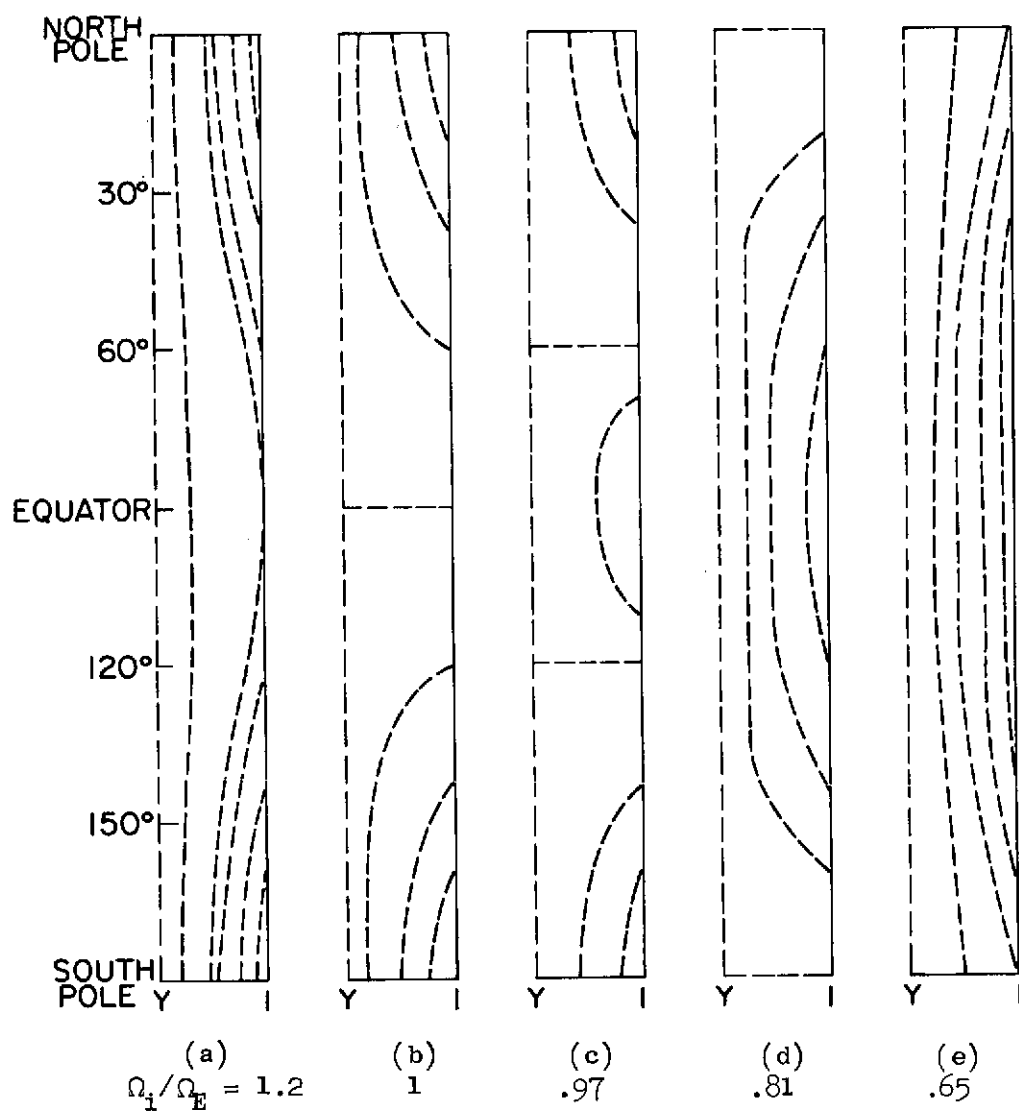
79

Figure 5. Contour lines of the angular velocity in the region with thermomechanical effect for different values of Ω_i.

Table 3

SERIES REPRESENTATION OF THE ROTATION PATTERN OF THE PARTIALLY IONIZED TOP LAYERS OF THE SUN

ℓ	$\Omega = \displaystyle\sum_{\ell=1}^{4} C_\ell R_\ell(r)\,\Theta_\ell(\theta)$		
	C_ℓ	$R_\ell(r)$	$\Theta_\ell(\theta)$
1	Ω_i	$\dfrac{Y^3/r^3 - Y^3}{1 - Y^3}$	1
2	$\Omega_0 + \dfrac{1}{5}\Omega_2 + \dfrac{3}{35}\Omega_4$	$\dfrac{1 - Y^3/r^3}{1 - Y^3}$	1
3	$\dfrac{4}{5}\Omega_2 + \dfrac{8}{15}\Omega_4$	$\dfrac{r^2 - Y^7/r^5}{1 - Y^7}$	$\dfrac{5\cos^2\theta - 1}{4}$
4	$\dfrac{8}{21}\Omega_4$	$\dfrac{r^4 - Y^{11}/r^7}{1 - Y^{11}}$	$\dfrac{21\cos^2\theta - 14\cos^2\theta + 1}{8}$

rate at the inner boundary, Ω_i. Of these, Y expresses the thickness of the part of the convection zone with significant partial ionization. As noted in the introduction to this chapter, for the present sun this would either be the top 35,000 km of the convection zone where helium gradually de-ionizes, or the top 7,000 km where the de-ionization of hydrogen comes into play. It is certainly true that the latter has the more drastic effect on the thermodynamic properties of the convective material. Moreover, there is direct evidence for the formation of closed vortex lines in this region in the form of the supergranulation. On the other hand, a global circulation as required for the equatorial acceleration will more readily develop in a thicker layer. In the framework of the present theory we are not able to decide from available observational data whether the region with latitude dependency should comprise the top 5% or the top 1% of the solar layers.

A second uncertainty is introduced by the unknown rotation rate at the bottom of the region with latitude-dependent rotation. The structure of the rotation pattern differs critically for cases where the interior rotation rate is higher than the equatorial rotation rate, lower than the polar rotation rate or in between those. The differences may be illustrated graphically by means of the contour lines of the angular velocity in a meridional plane, as in Fig. 5 for the following five cases:

(a) $\Omega_i = 1.2\ \Omega_E$ (fig. 5a)

If the interior rotation rate exceeds the equatorial rotation rate at the surface then the angular velocity increases inward everywhere. Starting on one side of the polar axis, some of the contour lines reach the other side uninterrupted and some terminate on the outer surface. The radial gradients of the angular velocity are largest near the poles.

(b) $\Omega_i = \Omega_E$ (fig. 5b)

If the interior and equatorial angular velocity are equal, then there is an inwardly increasing angular velocity except at the equator. All the contour lines beginning on the polar axis end on the outer surface. The contour line representing the interior rotation rate has a branch point at the equator.

(c) $\Omega_i = .97\ \Omega_E$ (fig. 5c)

If the interior rotation rate is anywhere between the equatorial and the polar rates then the radial angular velocity gradient changes sign at that latitude where the interior rotation rate equals the surface rotation. For the present case the angular velocity decreases inward at latitudes below 30° and increases inward at higher latitudes. This interesting feature might be connected with the various anomalies which have recently been ascribed to this latitude. There are now two branch points in the contour for the interior rotation at the critical latitudes where the angular velocity does not depend on radius.

(d) $\Omega_i = .81\ \Omega_E = \Omega_p$ (fig. 5d)

If the interior rotation rate is equal to the polar rotation rate at the surface then the angular velocity decreases inward everywhere except on the polar axis, where it is constant. All contour lines begin and end on the outer surface, including the one for the interior rotation rate, which is now without branch point. The radial shear is largest in the equatorial regions.

(e) $\Omega_i = .65\ \Omega_E = .8\ \Omega_p$ (fig. 5e)

This case is the reverse of case (a), with the angular velocity decreasing inwards everywhere, and some contours beginning and ending on the polar axis, some beginning and ending on the solar surface.

In order to develop a preference for one of the above described rotation patterns we have to revert to evidence of a more circumstantial nature than has been used so far. In the first place, there is the argument based on the east-west-asymmetry of sunspot numbers that in the sunspot region the angular velocity would decrease inward. This would rule out the cases (a) and (b). Another consideration comes from the helicity observed in chromospheric whirls. On the sun both types of helicity may be found on either hemisphere. The sense of the helicity is thought to depend on the sign of the radial angular velocity gradient. In the solutions c, d, e this gradient is opposite above and below the inner boundary of the top layer. In the process of breaking through this layer a magnetic flux tube could either retain its initial helicity, or it could be reversed because of the opposite radial shear. A fairly thin top layer would seem to be required for this explanation of the helicities of chromospheric whirls.

For Leighton's model of the solar cycle an inwardly increasing angular velocity is required. In our solution, this is the case below the layers with partial ionization, but not above these in the solutions c, d, e. However, if the top layer is thin enough, this would not affect the field amplification seriously until field eruption takes place.

The above arguments seem to leave us with a rotation pattern of the type c, d or e. Of these, the solution (c) represents the smallest

deviation from the pattern which would be there in the absence of a meridional circulation. It would seem safest to assume that the effect of this circulation is indeed small. In case (c) the rotation pattern in the polar regions is virtually unchanged by the meridional circulation. Only at low latitudes does the circulation make its presence felt by way of reversing the sign of the angular velocity gradient from its sign at higher latitudes in the top layer and everywhere outside the region with partial ionization. In summary, we may say that the above circumstantial evidence points at an equatorial acceleration caused by the de-ionization of hydrogen, and that the bottom of this layer has a slightly lower rotation rate than on the surface at the equator.

VI LOCAL SOLUTIONS

In the preceding chapter we obtained analytic solutions of the pro-
posed equation for convective heat transfer for the convection zone as a
whole. This solution led to the view that in the convective layers with
partially ionized hydrogen a thermally driven meridional circulation exists
stretching from the poles to the equator. Whereas the surface velocities
of this global circulation are too low for observational verification,
there are numerous observations which reveal local flow patterns indicat-
ing the presence of local circulations underneath the surface of the con-
vection zone. These local flow patterns subdivide into two categories.
The longest known of these is a radial outflow observed in sunspot penum-
bras throughout their existence. This type is called the Evershed-flow,
after its discoverer. The second and more recently discovered category is
a network of polygons covering the entire solar surface. In each individ-
ual polygon the solar material is observed to flow away from the center and
towards the edges. This flow pattern is called the supergranulation. As
early as 1913 St. John interpreted the Evershed flow as the surface mani-
festation of an underlying vortex ring surrounding the vertical magnetic
flux tube of each sunspot umbra below the solar surface. An analogous
interpretation of the supergranulation as a network of convective cells
has found wide acceptance. We will now proceed to discuss the bearing of
the present theory of convective heat transport on the local circulations
in the solar convection zone.

From our discussion of the solar rotation a picture of the convection
zone emerged which was divided into a large region with vanishing thermo-
mechanical effect and a small region with non-vanishing thermomechanical
effect. The latter region was argued to coincide with the layers where
the partial ionization of hydrogen is significant, i.e. the top 10,000 km
of the convection zone. According to the present theory, convective heat
transfer in this region has to be accompanied by the formation of closed

vortex lines. With regard to the structure of the ensuing circulations, the presence of an external rotation will make a crucial difference by introducing a preferred direction into the problem. In a rotating convective envelope the spins of individual convective parcels remain alligned with the external rotation vector. This is a basic feature of the "expanding sphere" model for convective parcels adopted in Chapter IV. The proposed equation for convective heat transfer is a direct consequence of this model. The external rotation organizes the individual spins in patterns leading to a global circulation rising at the poles and sinking at the equator.

In the absence of external rotation, the situation is essentially different. There is no external agency which organizes the spins of individual convective parcels into patterns which can transfer heat systematically. The rotational instability described in Chapter IV leads to spins which are randomly oriented in horizontal planes. In spite of this, the supergranulation and the Evershed flow bear out the existence of ordered spin patterns below the surface. In both cases the length scale of this order remains close to the thickness of the layer with thermomechanical effect. For the local circulations, the cause of the order must be looked for in the forces which the spins of individual convective parcels exert on one another. In the above cases the global "induced ordering" of spins by an external rotation corresponds to induced magnetization for para- or diamagnetic materials, whereas "spontaneous ordering" corresponds to spontaneous magnetization which occurs in various types of ferromagnetic materials.

As a result of the unknown nature of the internal spin forces we can establish neither the proportionality of the spin- and vorticity fields, nor the constancy of their proportionality factor. Whereas in the presence of external Coroilis forces these features follow immediately from the "expanding sphere" model of convective parcels, it is not at all clear what bearing this model has on the internal interaction of spinning convective parcels. Yet the linear relation between the vorticity and spin field still has the merit of simplicity and analytical tractability. We will therefore adhere to its validity in the remainder of this chapter. This will enable us to obtain analytical descriptions of the local circulations under consideration, whereby the above hypothesis may be tested against the available observational data.

If the applicability of the proposed rotational equation of state to non-rotating situations is open to doubt, the further procedure leading to our equation for convective heat transfer is warranted by the observations. As seen in Chapter IV, the central assumption of this procedure is that the solar convection zone is in a state of convective equilibrium characterized by minimum dissipation of energy. For the convection zone as a whole, this principle is borne out by the spherical shape and uniform temperature distribution of the solar surface. Similarly, on the local scale the uniformity of the temperature and the flatness of the surface attest to the high degree to which minimum dissipation is maintained on the supergranular and penumbral level. Deviations from uniformity and flatness start to occur only in structures which are about an order of magnitude smaller than the local circulation as a whole. For individual supergranular cells, this is all the more striking because of their relatively short lifetime of approximately 20 hours. In penumbral regions a much longer period of typically several weeks is available for setting up convective equilibrium. In this case the characteristic sharp edges with the umbral region and with the surrounding photosphere bear out the prevalence of convective equilibrium throughout the existence of the spot.

The methods for finding the flow patterns of the local circulation analogous to those for the global circulation described in the previous chapter, with the spherical geometry now replaced by a cylindrical geometry. Assuming axial symmetry, the vorticity can first be found from the known form of the heat flux below the surface. As with the global circulation, the local circulations are wrapped in surface currents of heat which match the discontinuities in the vorticity which occur on their surfaces. Similarly, the stream functions of the local circulations obey differential equations which allow stable solutions only for certain types of boundary conditions. We will now proceed to investigate the analytic form of the local circulations underlying the supergranulation and the Evershed flow as resulting from the observational data collected in Chapter II and the equation for convective heat transfer derived in Chapter IV.

VI.1 Supergranulation.

Before the flow pattern of individual supergranular cells can be calculated two approximations regarding their structure have to be made. The close packing of supergranules over the entire solar surface leads to a polygonal horizontal cross section of them which is best approximated by a hexagon. Because a hexagonal cell lacks axial symmetry, this geometry is not convenient for the integration of our equation for convective heat transfer. For this reason we approximate the vertical boundary of the supergranule by a cylinder and impose axial symmetry about the axis of this cylinder.

As a second approximation we neglect the curvature of the horizontal boundaries of the supergranule. This is reasonable because the typical horizontal length scale of supergranules of about 32,000 km is less than 5% of the solar radius. Thus the supergranular flow takes place inside a vertical circular cylinder bounded by two horizontal planes. For the distance between these planes we take the thickness of the region with thermo-mechanical effect, or about 16,000 km. This means that the vertical cross section of the supergranule is a rectangle whose horizontal sides are twice as long as its vertical sides.

For the description of the flow pattern we adopt a rectangular coordinate frame with the polar axis along the symmetry axis of the supergranule. The zero level of the polar axis is taken at the upper surface, with the positive direction pointing downward. Thus in cylindrical coordinates ρ, φ, z the surface of the sun is at $z = 0$. The lower horizontal boundary of the supergranule is taken at $z = L$ and the vertical boundary has a radius $\rho = a$. As stated above we have adopted for the aspect ratio of the cylinder a value $a/L = 1$.

VI.1.1 Normal Modes of the Azimuthal Velocity.

Because of the external rotation of the supergranular network each local circulation will experience a Coriolis force which will bring about a cyclic flow around the symmetry axis of the cell. Thus throughout each supergranule an azimuthal component of the velocity field should be present.

For the present case a normal mode expansion for the azimuthal velocity can be obtained along the same lines as in Chapter V for the global rotation.

The principle of least dissipation rules out the presence of an azimuthal component of the heat flux. Then Equation IV.27a for the convective heat transfer leads to a partial differential equation for the azimuthal velocity which can be solved immediately by separation in cylindrical coordinates ρ, z. The resulting equations can be solved either in terms of ordinary Bessel functions for the ρ-dependence and exponentials for the z-dependence, or, alternatively in terms of modified Bessel functions, combined with sines and cosines, viz.:

$$\left[\frac{1}{\rho}\frac{\partial}{\partial\rho}\rho\frac{\partial}{\partial\rho} - \frac{1}{\rho^2} + \frac{\partial^2}{\partial z^2}\right]v_\varphi = 0 \qquad (1a)$$

$$v_\varphi = \begin{cases} \sum_k J_1(k\rho)\left\{A_k e^{kz} + B_k e^{-kz}\right\} \\ \sum_k I_1(k\rho)\left\{C_k \sin kz + D_k \cos kz\right\} \end{cases} \qquad (1b)$$

In the solutions (1b) only Bessel functions of the first kind appear in order to avoid infinite velocities on the symmetry axis $\rho = 0$. In the first representation (1b) the nodal surfaces of each mode are cylinders coaxial with the symmetry axis, whereas in the second representation (1b) the nodal surfaces are horizontal planes.

For a complete determination of the azimuthal flow pattern the boundary conditions on the azimuthal velocity have to be invoked. As for the spherical case of Chapter V, the azimuthal velocity is continuous on the surface, but its normal derivative may suffer a discontinuity which is matched by a surface current of heat. As noted in Chapter II, any azimuthal velocities on the observable surface of supergranules are below the present limits of detectability. This condition can be met with the solutions (1b) without ruling out significant azimuthal velocities in the interior of the cell. On the other hand, such a cyclic flow pattern requires a dissipative surface current to match it to the surrounding fluid. This

surface dissipation will keep the azimuthal velocities at the negligible level which they have on the observable surface of each supergranule.

VI.1.2 Azimuthal Vorticity.

As a first step towards finding the structure of the local circulation the analytic form of the heat flux inside the supergranule has to be found. In view of the even temperature distribution and the levelness of the observable surface the heat flux below the surface may be taken as uniform and purely vertical. This is consistent with the absence of sources or sinks of heat, and with the neglect of curvature. The vanishing of the divergencies of the heat flux vector $\vec{q}$ and of the vector $\vec{cq}$ implies that the constant c for the thermomechanical effect does not depend on z. c is also assumed independent on distance from the symmetry axis because the thermodynamical state of the solar material is for the present case the same on horizontal surfaces. With these assumptions, Equation IV.27a can be integrated with Stokes' theorem over a horizontal circular loop centered on the symmetry axis of the supergranule. The result is that the azimuthal component of the vorticity increases linearly with distance from the symmetry axis, viz.:

$$\frac{1}{\rho} \frac{\partial}{\partial \rho}(\rho w_\varphi) = cq_\odot \tag{2a}$$

$$w_\varphi = \frac{1}{2}cq_\odot\rho \tag{2b}$$

The vertical heat flux $q_\odot$ may be taken equal to the energy flux at the solar surface. The solution (2b) constitutes a circulation which for positive c rises in the center and sinks at the edges of the cell. Thus a positive thermomechanical effect corresponds to the observed sense of the local circulation. This conforms with the positive thermomechanical effect which was inferred in Chapter V in connection with the equatorial acceleration.

Because the local circulation (2b) is sandwiched between two layers which do not admit closed vortex lines, there are discontinuities in the azimuthal vorticity at the top and bottom surface of the cell. These

discontinuities are matched by radial surface currents of heat, which for positive c are pointed outward at the top surface and inward at the bottom surface of the cell. At the vertical boundary a single isolated cell would have a uniform downward surface current matching the transition from non-zero to zero azimuthal vorticity. Adjacent cells will locally increase this downward current sheet. The formulas for the above surface currents are from Equations IV.27a and VI.2b:

$$\text{at } \rho = a \; : \quad K_z = \frac{1}{2}q_\odot a \tag{3a}$$

$$\text{at } z = o, L \; : \quad K_\rho = \pm \frac{1}{2}q_\odot \rho \tag{3b}$$

The surface currents allow the local circulation (2b) to exist embedded in a region with vanishing vorticity.

VI.1.3 Stream Function.

For the further elucidation of the flow pattern it is again convenient to revert to the stream function. In this respect the remarks made in the previous chapter with respect to the existence of stable solutions for the stream function carry over directly to the present cylindrical geometry. That is, in the framework of the present theory neither the global nor the local circulations can be stable. The observations on the supergranulation provide a direct illustration of this result: with surface velocities in the order of .3-.5 km/sec the 20-hour lifespan of an average supergranule is too short to allow the supergranular material even only one full round trip along its 96,000 km circumference.

It is still possible to obtain a general impression of the structure of the local circulations by relaxing the rigorous boundary conditions which the present theory imposes on the stream function. Specifically, if the condition that both the horizontal and the vertical component of the velocity vanishes at the bottom surface of the cell is replaced by the condition that either the vertical or the horizontal component vanishes there, then an analytic solution for the stream function becomes possible. For this it is also necessary that the flow is incompressible. For the observable

part of supergranules this is a reasonable assumption, because the observed surface velocities are much smaller than the local speed of sound. In the interior of the cell this condition will have to be verified retrospectively after the solution for the flow pattern has been obtained.

In an axially symmetric situation the continuity equation for incompressible flow and its solution in terms of the stream function ψ take the form in cylindrical coordinates ρ, φ, z:

$$\frac{1}{\rho} \frac{\partial}{\partial \rho}(\rho v_\rho) + \frac{\partial v_z}{\partial z} = 0 \tag{4a}$$

$$v_\rho = \frac{1}{\rho} \frac{\partial \psi}{\partial z} , \quad v_z = \frac{-1}{\rho} \frac{\partial \psi}{\partial \rho} \tag{4b}$$

In Equations (4) and in the following the coordinate ρ denoting the distance from a point to the symmetry axis of the cell should not be confused with the symbol ρ of the previous chapter, which denoted the mass density of the fluid. On substituting Equation (4b) in the expression for the azimuthal vorticity (2b) a second order partial differential equation for the stream function is found. This differential equation is of the elliptic type and hence yields a unique stable solution of the values of the stream function or of its normal derivatives are given on a closed surface. A free surface is represented by a vanishing stream function there. This is the proper boundary condition for the top surface and for the vertical cylinder bounding the supergranular cell. On the bottom surface both ψ and its normal derivative have to vanish in order to have neither radial nor vertical velocities there. Since this combination of boundary conditions leads to unstable solutions for the stream function, the two conditions on the bottom surface are imposed separately. In this way we obtain the following two systems:

$$\left[\rho \frac{\partial}{\partial \rho} \frac{1}{\rho} \frac{\partial}{\partial \rho} + \frac{\partial^2}{\partial z^2} \right] \psi = \frac{1}{2} c q_\odot \rho^2 \tag{5a}$$
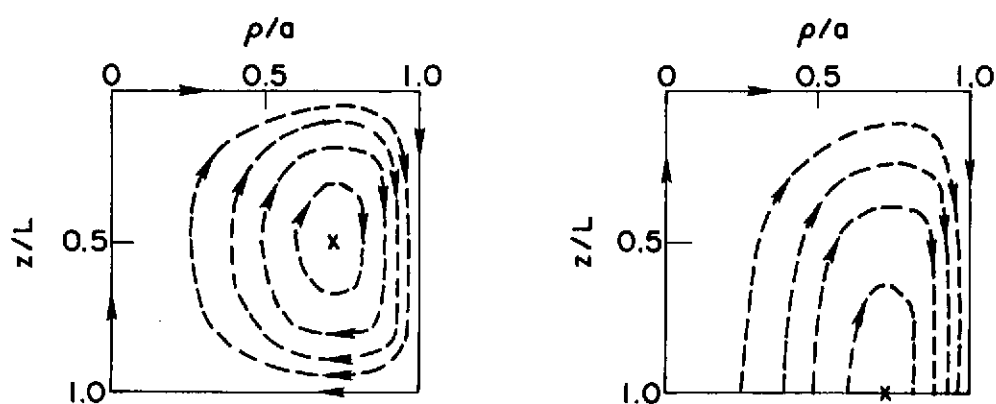
(i) at $\rho = a, z = 0, L : \quad \psi = 0$ \hfill (5b)
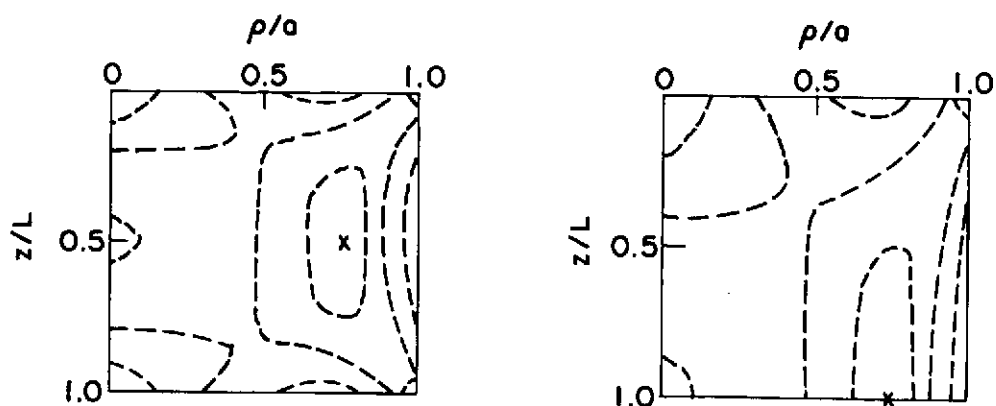
(ii) at $\rho = a, z = 0 : \quad \psi = 0$

at $z = L : \quad \frac{\partial \psi}{\partial z} = 0$ \hfill (5c)
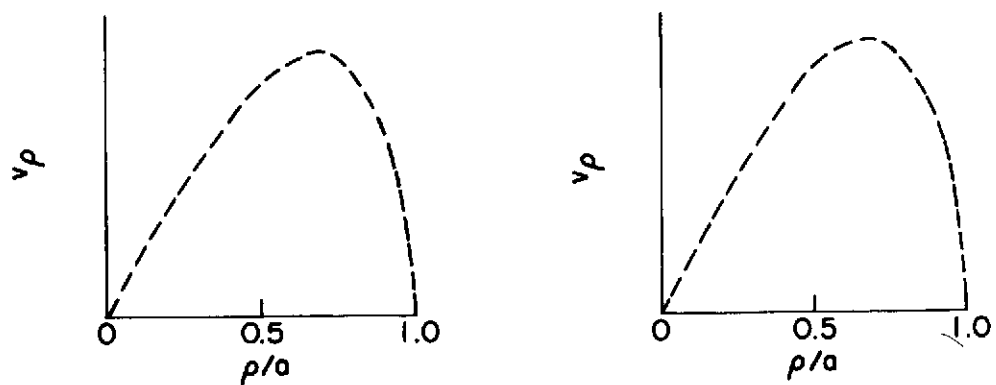
(a) Surface velocities

(b) Streamlines

(c) Contour lines of the velocity

Figure 6. Flow pattern of the supergranular vortex ring in vertical planes through the symmetry axis.

93

The solution of the systems (5) can be effected with the theory of Green's functions in terms of the functions which describe the normal modes of the azimuthal velocity, Equation (1b). For the boundary conditions (5b) the solution takes the forms

$$\psi = \begin{cases} cq_{\odot}a\rho \sum_{n=1}^{\infty} \dfrac{J_1(s_n\frac{\rho}{a})}{s_n^3 J_2(s_n)} \left\{ 1 + \dfrac{\cosh(s_n\frac{L}{a})-1}{\sinh(s_n\frac{L}{a})} \sinh(s_n\frac{z}{a}) - \cosh(s_n\frac{z}{a}) \right\} & (6a) \\[4ex] \dfrac{2cq_{\odot}aL^2}{\pi^3} \rho \sum_{n=1,3,\ldots}^{\infty} \left\{ \dfrac{\rho}{a} - \dfrac{I_1(\frac{n\pi\rho}{L})}{I_1(\frac{n\pi a}{L})} \right\} \sin(\dfrac{n\pi z}{L}) & (6b) \end{cases}$$

In the first representation (6) s_n denotes the n-th zero of the Bessel function J_1. This takes care of the boundary condition at $\rho = a$.

The structure of the flow pattern described by the stream function (6) is illustrated graphically in Figure 6. In the left column of Figure 6 the surface velocity, the stream lines and the contour lines of the velocity have been represented. In each case the first twenty terms of each series representation in (6) were taken. This gave numerical values agreeing to within a few percent.

The overall picture of the flow pattern is as might have been expected. Inside the supergranular cell a vortex ring exists with a heart line half way between the top and bottom surfaces and at 70% distance from the axis. As evident from Figures 6b,c the highest velocities occur on the surfaces nearest to the heart line of the vortex ring, with the vertical downward velocities somewhat higher than the peak velocities on the horizontal boundaries. The lowest velocities occur near the heart and near the corners of the vortex ring. On the top surface, the radial outward velocity first increases approximately linearly with distance from the symmetry axis, then peaks at about 70% of the cell radius and drops off rapidly to zero again (Figure 6a).

The flow pattern belonging to the alternative mixed boundary conditions (5c) can be obtained immediately by noting the symmetry of the solution (6) about the plane $z = L/2$. As illustrated by the form of the

stream lines in Figure 6b, there are no radial velocities at the level
z = L/2. By stretching out the solution (6) in the z-direction by a factor
of two, the radial velocity can be made to vanish on the z = L level in-
stead. The solution then automatically obeys the mixed boundary conditions
(5c). The flow pattern of this case is illustrated in the right-hand col-
umn of Figure 6. A comparison of Figure (6a) shows that in the new case
the surface velocity has a slightly higher peak value. The figure allows
us to conclude that the boundary conditions at the bottom of a supergranule
have remarkably little effect on the velocities produced on the upper sur-
face of a supergranular cell.

VI.2 Evershed Flow.

As noted in the introduction to the present chapter, there is a second
type of local flow on the surface of the solar convection zone, different
from the supergranulation. This is the predominantly radial outward flow
of solar material found in sunspot penumbras, and known as the Evershed
flow. The similarities and differences of the two types of flow are several.
We have adopted the view that both types of flow are surface manifestations
of an underlying vortex ring, with the supergranular vortex ring confined
by a vertical cylinder and two horizontal planes and the penumbral vortex
ring confined by two vertical coaxial cylinders and two horizontal planes.
In both cases the horizontal planes represent the top and bottom of the
layer with thermomechanical effect; for the penumbral vortex ring the inner
cylinder represents the boundary with the vertical umbral magnetic flux
tube and the outer cylinder represents the boundary with the unperturbed
supergranular network. This model applies to single spots with a fairly
circular horizontal cross section.

In contrast with the supergranular flow, the Evershed flow is steady.
The outward flow in penumbras continues without interruption throughout
the lifetime of the sunspot. This may amount to several months for large
spots, as compared to a 20-hour lifespan for an average supergranule. In
the present theory the stability or instability of a circulation is traced
back to the boundary conditions. For the supergranulation the condition
that the velocity vanish at the lower boundary was found to preclude the
formation of a steady circulation. This boundary condition has to be dropped
for the present case, if the Evershed flow is to be the surface manifesta-
tion of an underlying penumbral circulation. The presence of strong mag-
netic fields inhibiting the convective momentum exchange provides a rationale
for this modification.

Although the dimensions of average sunspots are comparable to those
of supergranules, the penumbral velocities are larger by as much as an
order of magnitude. The penumbral flow may also have a significant azi-
muthal component.

One aspect of the penumbral structure noted in Chapter II will not be
incorporated in the present description of the Evershed flow. This is the

apparent depression of the sunspot umbra with respect to the photospheric
level, known as the Wilson effect. Because of this depression, the penum-
bral surface is not flat and horizontal, but actually more of a conical
nature. Since this deviation generally does not amount to more than a few
degrees, it is neglected in the following discussion.

VI.2.1 Normal Modes of the Azimuthal Velocity .

The differential equation for the normal modes of the azimuthal ve-
locity inside the penumbral vortex ring follows at once from the equation
for convective heat transfer IV.27a by assuming that there is once again
no azimuthal heat flux. This is again in compliance with the principle
that the penumbral region is in a state of convective equilibrium charac-
terized by minimum dissipation. The general solution for the differential
equation for the azimuthal velocity now contains first order Bessel func-
tions of both kinds because the symmetry axis of the circulation is now
excluded from the region where the flow takes place. We have, in cylindri-
cal coordinates ρ, φ, z:

$$\left[\frac{1}{\rho} \frac{\partial}{\partial \rho} \rho \frac{\partial}{\partial \rho} - \frac{1}{\rho^2} + \frac{\partial^2}{\partial z^2} \right] v_\varphi = 0 \tag{7a}$$

$$v_\varphi = \begin{cases} \sum_k \left\{ A_k J_1(k\rho) + B_k Y_1(k\rho) \right\} \left\{ C_k e^{kz} + D_k e^{-kz} \right\} \\[2ex] \sum_k \left\{ P_k I_1(k\rho) + Q_k K_1(k\rho) \right\} \left\{ R_k \sin(kz) + S_k \cos(kz) \right\} \end{cases} \tag{7b}$$

Owing to the oscillatory nature of the ordinary Bessel functions J_1, Y_1
the nodal lines of the normal modes of the first series expansion (7b) are
again cylinders coaxial with the symmetry axis, whereas the sines and co-
sines in the second expansion (7b) give nodal surfaces in the form of hori-
zontal planes.

Various types of boundary conditions can be met with the integration
constants in (7b) and with the summation index. As was said in the previous
section, we have opted for free surfaces at all boundaries of the penumbral
vortex ring. On only one of the boundaries can the azimuthal flow be found

from observations. This is insufficient to determine the constants occur-
in the series representations (7b). In the present formulation the azi-
muthal velocity field below the penumbra cannot be obtained from observed
azimuthal surface velocities. This is not a serious shortcoming because
the radial surface velocities are generally much larger than the azimuthal
velocities, to an extent that the latter are in many spots altogether unde-
tectable.

VI.2.2 <u>Azimuthal Vorticity</u> .

A general impression of the flow pattern due to the radial and verti-
cal velocities is afforded by integration of Equation IV.27a with Stokes'
theorem, leading to an expression for the azimuthal vorticity. Again the
heat flux is assumed uniform and vertical, and the thermomechanical effect
is assumed constant throughout the penumbral region. The contour of inte-
gration is again a horizontal circular loop centered on the symmetry axis,
and the surface of integration is the planar region bounded by this contour.
Thus the surface integration extends over both penumbral and umbral regions.
The absence of radial velocities in sunspots umbras indicates that the strong
vertical umbral magnetic fields prohibit the formation of an underlying vor-
tex ring. This implies that in the umbral regions the rotational heat flux
is suppressed. It is of course tempting to ascribe the observed tempera-
ture difference between sunspot umbras and unperturbed photosphere to this
suppression. Analogously, the intermediate temperature of the penumbra
would be due to an inhibition of the rotational heat flux stemming from the
inner boundary. This interpretation would imply that nearly three quarters
of the heat flux in the layer with thermomechanical effect is carried rota-
tionally.

For our present purposes it is sufficient to assume that the thermo-
mechanical effect vanishes in the umbral region and is constant throughout
the penumbral vortex ring. The integration of Equation IV.27a with Stokes'
theorem over the above described surface then gives an azimuthal vorticity
which now comprises both a linear and a hyperbolic dependence on distance
from the symmetry axis, viz.:

$$\frac{1}{\rho}\frac{\partial}{\partial\rho}(\rho w_\varphi) = cq_p \qquad (8a)$$

$$w_\varphi = \frac{1}{2}cq_p(\rho - \frac{a^2}{\rho}) \qquad (8b)$$

In Equation (2) q_p is the penumbral heat flux, which is typically about 20% below the corresponding photospheric value. The solution (2b) ascertains that at the boundary of the umbra and the penumbra $\rho = a$ the azimuthal vorticity vanishes, in compliance with the absence of a thermomechanical effect in the umbral region. The sense of the circulation again bears out a positive thermomechanical effect.

As for the earlier circulations, the penumbral vortex ring is wrapped in surface currents of heat matching the discontinuities in the azimuthal vorticity which the solution (8b) implies there. For the present case, the one surface without such a discontinuity is the boundary with the umbral regions. On both sides of this boundary the azimuthal vorticity is zero. The current sheets on the remaining boundaries follow directly from Equation (2b) and take the form:

$$\text{at } \rho = b : \quad K_z = \frac{1}{2}q_p(b - \frac{a^2}{b}) \qquad (9a)$$

$$\text{at } z = o, L : \quad K_\rho = \pm \frac{1}{2}q_p(\rho - \frac{a^2}{\rho}) \qquad (9b)$$

The boundary of the penumbra with the surrounding photosphere has been taken at radius $\rho = b$. At this interface, the surface current is downward, at the top and bottom surfaces it is outward and inward respectively, consistent with the general sense of the circulation.

VI.2.3 Stream Function.

For the detailed structure of the penumbral vortex ring we once again resort to the stream function. It is then necessary to assume that the flow is incompressible. This is open to more doubt than for the supergranular flow, because of the higher velocities observed in the Evershed flow. In the deepest observable layers of the penumbra the outward velocities may reach several kilometers per second. This compares to a local speed of
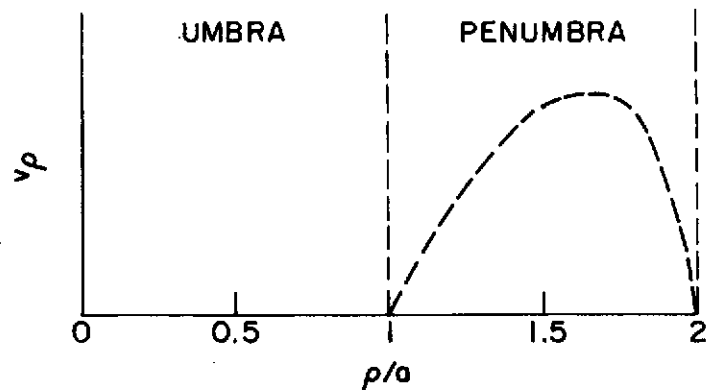
(a) Surface velocity
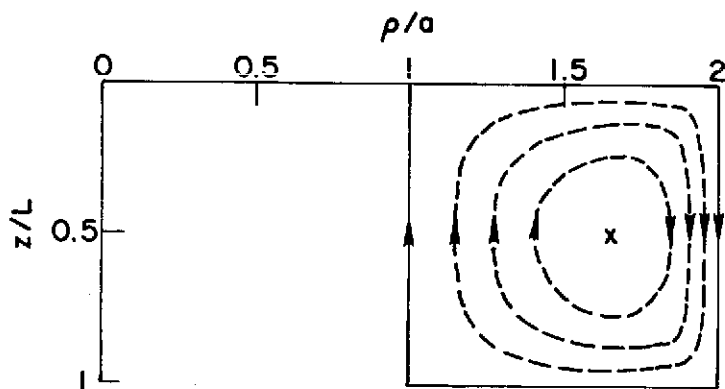
(b) Streamlines
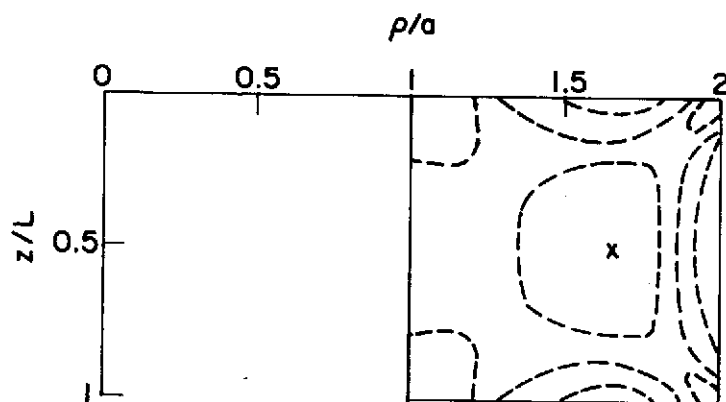
(c) Contour lines of the velocity

Figure 7. Flow pattern of the penumbral vortex ring in vertical planes through the symmetry axis.

100

sound of about 6-10 km/sec in these regions. From our experience with the supergranular flow we may anticipate that the highest velocities again will occur on the boundaries. In that case the incompressibility condition will be met with increasing accuracy in the lower layers of the penumbral vortex ring because of the rapid downward increase in temperature and the concomitant increase in local speed of sound.

The stream function is defined in terms of the radial and vertical components of the velocity as given in Equation (4b). The partial differential equation for the stream function is only different from Equation (5a) as regards the inhomogeneous term, whose parabolic radial dependence is now shifted over a distance equaling the inner penumbral radius. In connection with the required steady solution, we have opted for free surfaces on all boundaries. The stream function is then subject to the system:

$$\left[\rho \frac{\partial}{\partial\rho} \frac{1}{\rho} \frac{\partial}{\partial\rho} + \frac{\partial^2}{\partial z^2}\right] \psi = \frac{1}{2}cq_p(\rho^2 - a^2) \tag{10a}$$

$$\text{at } \rho = a,b; \ z = o,L : \ \psi = 0 \tag{10b}$$

The solution of Equations (10) can again be effected in terms of the functions found in connection with the normal modes of the azimuthal velocity, Equation (7b). For our present purposes the representation in modified Bessel functions and sines is the more convenient one. The alternative representation requires the determination of a set of zeros which depend on the ratio of the umbral and penumbral radii. In terms of modified Bessel functions and sines, the solution of Equations (10) for the stream function takes the form:

$$\psi = \frac{2cq_p aL^2}{\pi^3}\rho \sum_{n=1,3,\dots}^{\infty} \frac{1}{n^3} \left\{ \frac{\rho}{a} - \frac{a}{\rho} - (\frac{b}{a} - \frac{a}{b}) \times \right.$$

$$\left. \times \frac{K_1(\frac{n\pi a}{L})I_1(\frac{n\pi\rho}{L}) - I_1(\frac{n\pi a}{L})K_1(\frac{n\pi\rho}{L})}{K_1(\frac{n\pi a}{L})I_1(\frac{n\pi b}{L}) - I_1(\frac{n\pi a}{L})K_1(\frac{n\pi b}{L})} \right\} \sin(\frac{n\pi z}{L}) \tag{11}$$

101

In the limit a → 0 the expression (11) reduces to the expression (6b) found for the supergranular circulation. The stream function describing the supergranular flow pattern is a special case of the more general stream function (11) describing the penumbral circulation.

The general structure of the penumbral vortex ring is illustrated in Figures 7a,b,c. The figures pertain to a fairly large sunspot with 16,000 km umbral radius. The outer penumbral radius is taken twice as large. The radial outward velocity starts at zero at the boundary of the umbra and the penumbra, reaches a maximum at 2/3 of the umbral width and returns to zero again at the outer penumbral radius. The surface velocity thus peaks well within the penumbral region. As noted in Chapter II, this behaviour has been found in large spots. For smaller spots the maximum appears to be closer to the outer penumbral edge than Figure 7a indicates. It should of course be remembered that even the deepest layers in which the Evershed flow is observed are not a part of the actual convection zone to which the solution (11) applies. The first absorption lines are formed well above the level where convection has ceased to be the dominant form of energy transfer. For this reason the possible extension of the outflow beyond the penumbra is not incompatible with the present solution, in which the outflow of the convectively-controlled surface layers is strictly confined to the penumbral region. The penumbral vortex ring must be looked at as providing the basic moving force for the Evershed flow; the various photospheric and chromospheric manifestations of this flow are of course strongly influenced by conditions outside the realm of the convection zone.

From the structure of the stream lines it is clear that again the highest velocities occur on the boundaries of the penumbral vortex ring; towards the heartline the circulation becomes slower and slower. This behavior is also illustrated with the contour lines of the velocity in Figure 7c. At each of the corners of the vortex ring the velocity vanishes completely. The penumbral circulation differs only in quantitative details from the structure of the supergranular circulation illustrated in Figure 6. One such difference is that the heartline of the penumbral vortex ring lies more closely halfway between the vertical boundaries. This will be due to the larger radius of curvature of the outer bounding surface in the present case.

APPENDIX A. BUOYANCY-INDUCED SPIN

This appendix comprises a derivation of equation IV.3 for spin due to
rotational instability of superadiabatic fluid layers along the lines of
the textbook derivation for velocity due to translational instability in
mixing length fluids. Consider a fluid with temperature T and density ρ
at rest in a gravitational field $\vec{g}$. An adiabatic motion of a fluid parcel
will in general perturb the density distribution and hence give rise to
buoyancy forces. For the special case of an adiabatic rotation a buoyancy
couple on the fluid parcel results. The subsequent rotational motion of the
parcel is then described by the balance of that buoyancy couple and the re-
sulting angular momentum rate of change:

$$\frac{d}{dt} \int \rho r^2 \vec{\omega} \ dV = \int (\rho_o - \rho) \ \vec{r} \times \vec{g} \ dV \tag{A.1}$$

where $\vec{r}$ denotes the position with respect to the center of mass of the
parcel, $\vec{\omega}$ the intrinsic rotation rate, ρ_o the initial value of the mass
density ρ and $\vec{g}$ the local acceleration of gravity. If the size of the
parcel is approximately equal to the local mixing length L then equation A.1
can be approximated in differential form as:

$$\frac{d\omega}{dt} \approx \frac{g\Delta\rho}{L\rho} \tag{A.2}$$

where we have introduced the density difference $\Delta\rho = \rho_o - \rho$. Equation A.2 for
the angular acceleration of a mixing length parcel is exact for a mass dis-
tribution in the form of a horizontal dumbell with bar length 2L. In the
standard mixing length theory $\Delta\rho$ is now replaced by its average value $\overline{\Delta\rho}$
between the formation and the dissolution of the parcel. Furthermore the
pressure distribution remains undisturbed. This implies that in an ideal gas
temperature and density fluctuations must compensate each other: $\Delta\rho/\rho = -\Delta T/T$,
and likewise for their average values. Assuming that the parcels rotate less
than $180°$ before dissolving, the average spin due to buoyancy couples can now
be estimated from the angular equation of motion A.2 to be:

$$\omega^2 \approx \frac{g\overline{\Delta T}}{LT} \quad . \tag{A.3}$$

This agrees with the result IV.3 obtained by substituting $\omega \approx v/L$ in the
Siedentopf-relation IV.2 for convective velocities in mixing length fluids.

APPENDIX B. VORTICITY-INDUCED SPIN

Consider a rotating horizontal layer of fluid in convective equilibrium described by the mixing length theory. The ratio of the pressure p of two points having one mixing length L vertical distance is:

$$\frac{p(z \pm L)}{p(z)} = \exp\left(\mp \frac{L}{H_p}\right) = \exp(\mp \alpha) \ . \tag{B.1}$$

The parameter α expressing the ratio of the local mixing length L to the local pressure scale height H_p is close to unity in standard mixing length theory. For fluid parcels undergoing adiabatic displacements pressure and volume are related by $pV^\Gamma = $ constant, where the first adiabatic index Γ is of order unity in normal gases. If the parcel is displaced over a vertical distance of one mixing length, and the concomitant volume changes are assumed to be spherically symmetric, then the initial and final pressure and the initial and final radius R are related by:

$$\frac{p(z \pm L)}{p(z)} = \left(\frac{V(z)}{V(z \pm L)}\right)^\Gamma = \left(\frac{R(z)}{R(z \pm L)}\right)^{3\Gamma} \ . \tag{B.2}$$

Because of the rotation of the layer each parcel is endowed with an intrinsic rotation rate or spin ω. For spherically symmetric volume changes the concomitant changes in moment of inertia of the parcel go as MR^2, where the mass M of the parcel is conserved. If the parcel is described in a corotating frame then the volume changes will produce coriolis couples which will set the parcel into a rotation with respect to the originally corotating frame. If the parcel is described in an inertial frame then it should conserve its angular momentum $MR^2\omega$ if other couples can be neglected. Thus the ratio of the final rotation rate $\omega(z \pm L)$ and the initial rotation rate $\omega(z)$ can be expressed directly in terms of the mixing length parameter α and the first adiabatic index Γ:

$$\frac{\omega(z \pm L)}{\omega(z)} = \left(\frac{R(z)}{R(z \pm L)}\right)^2 = \left(\frac{p(z \pm L)}{p(z)}\right)^{2/3\Gamma} = \exp \pm \frac{2\alpha}{3\Gamma} \tag{B.3}$$

where we have used equation B.2 and equation B.1 respectively. On identifying the initial rotation rate $\omega(z)$ with one half of the local vorticity equation B.3 becomes identical with the relations IV.5 setting the domain of the spin parameter.

REFERENCES

Abramowitz, M. and Stegun, I., Handbook of Mathematical Functions (Dover Publications, 1968).

Allen, C.W., Astrophysical Quantities (The Athlone Press, 1963).

Ananthakrishnan, R., Proc. Indian Acad. Sci. 40, 72 (1954).

Aslanov, I.A., Sov. Astron. AJ 7, 794 (1964).

Azambuja, L. and M.d', Ann. Obs. Meudon 6, facs. 7.

Baker, N. and Temesvary, S., Tables of Convective Stellar Envelopes (Second Edition, 1966).

Batchelor, G.K., Proc. Roy. Soc. A 201, 406 (1950).

Beckers, J.M., Sol. Phys. 3, 258 (1968).

Biermann, L., Zeitschrift für Astrophysik 28, 304 (1951).

Brekke, K. and Maltby, P., Ann. Astrophys. 26, 383 (1963).

Callen, H.B., Thermodynamics (John Wiley and Sons, 1966).

Carrington, R.C., Observations of the Spots on the Sun from November 9, 1853, to March 24, 1861 (London and Edinburgh: Williams and Norgate, 1863).

Chapman, S. and Cowling T.G., The Mathematical Theory of Non-Uniform Gases (Cambridge University Press, 1970).

Clayton, D.D., Principles of Stellar Evolution and Nucleosynthesis (McGraw-Hill, 1968).

Cocke, W.J., Ap. J. 150, 1041 (1967).

Cowling, T.G., The Sun (Univ. of Chicago Press, 1953), Ed. G.P. Kuiper, p. 551.

Dicke, R.H., Ann. Rev. Astron. Astrophys. 8, 297 (1970).

Durney, B.R. and Roxburgh, I.W., Sol. Phys. 16, 3 (1971).

Evershed, J., Mon. Not. R. astr. Soc. 70, 217 (1910).

Evershed, J., Mon. Not. R. astr. Soc. 69, 454 (1909).

Goldreich, P. and Schubert, G., Ap. J. 154, 1005 (1968).

Gough, D.O. and Lynden-Bell, D., J. Fluid Mech. 32, 437 (1968).

Grad, H., Comm. Pure Appl. Math. 5, 455 (1952).

Groot, S.R. de, The Maxwell Equations: Non-Relativistic and Relativistic Derivations from Electron Theory (North Holland Publishing Co., 1969).

Groot, S.R. de and Mazur, P., Non-Equilibrium Thermodynamics (North Holland Publishing Co., 1962).

Hale, G.E., Nature 119, 708 (1927).

Holmes, J., Mon. Not. R. astr. Soc. 126, 155 (1963).

Howard, R. and Harvey, J., Sol. Phys. 12, 23 (1970).

Jackson, J.D., Classical Electrodynamics (John Wiley and Sons, 1962).

Jager, C. de, Handbuch der Physik, Band LII (Springer-Verlag, 1959), p. 80.

Kinman, T.D., Mon. Not. R. astr. Soc. 112, 425 (1952).

Kippenhahn, R., Ap. J. 137, 664 (1963).

Köhler, H., Sol. Phys. 13, 3 (1970).

Kuiper, G.P., The Sun (University of Chicago Press, 1953).

Lamb, H., Hydrodynamics (Dover Publications, Sixth Ed., 1945).

Leighton, R.B., Noyes, R.W. and Simon, G.W., Ap. J. 135, 474 (1962).

Leighton, R.B., Ap. J. 156, 1 (1969).

Livingston, W.C., Sol. Phys. 9, 448 (1969).

Lury, R.E. de, JRAS Canada 33, 345 (1939).

Mamadazimov, M., Sol. Phys. 22, 129 (1972).

Mase, G.E., Continuum Mechanics (McGraw-Hill, 1970).

Maxwell, J.C., A Treatise on Electricity and Magnetism (Dover Publications, 1954).

Maunder, A.S.D., Mon. Not. R. astr. Soc. 67, 451 (1907).

Mestel, L., Stars and Stellar Systems 8, 465 (1965).

Mestel, L., Mem. Soc. Roy. Sci. Liege 19, 167 (1970).

Michard, R., Ann. Astrophys. 14, 101 (1951).

Minnaert, M.G.J., Mon. Not. R. astr. Soc. 106, 98 (1946).

Newton, H.W. and Nunn, M.L., Mon. Not. R. astr. Soc. 111, 413 (1951).

Nguen Van D'en and Listrov, A.T., Fluid Dynamics USSR 2, 87 (1971).

Noyes, R.W., IAU Symp. 28, 293 (1967).

Panofsky, W.K.H. and Phillips, M., Classical Electricity and Magnetism (Addison-Wesley, 1962).

Piddington, J.H., Sol. Phys. 21, 4 (1971).

Richardson, R.S. and Schwarzschild, M., Accademia Lincei, Convegno 11, Rome 1952, p. 228.

St. John, C., Ap. J. 37, 322 (1911).

Sakurai, T., Publ. Astron. Soc. Japan 18, 174 (1966).

Schröter, E.H., "The Evershed Effect in Sunspots" (in Solar Physics , Ed. Xanthakis, 1965).

Servajean, R., Ann. Astrophys. 24, 1 (1961).

Sheeley, N.R. and Bhatnagar, A., Sol. Phys. 19, 338 (1971).

Solonsky, Y.A., Sol. Phys. 23, 3 (1972).

Strittmatter, P.A., Ann. Rev. Astron. Astrophys. 7, 665 (1969).

Sturrock, P.A. and Gilvarry, J.J., Nature 216, 1280 (1967).

Tuominen, J., Z. Astrophys. 37, 145 (1956).

Wilcox, J.M. and Howard, R., Sol. Phys. 13, 251 (1970).